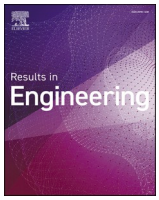
Results in Engineering 27 (2025) 106412



Contents lists available at ScienceDirect

Results in Engineering

journal homepage: www.sciencedirect.com/journal/results-in-engineering





Unravelling the sorption mechanism of two organic dyes (Indigo Carmine and Orange II) onto Al-Fum MOF: Kinetic and isotherm scrutinization

Albert-Yannick-Steve Mbega [a], Cyrille Ghislain Fotsop [b,e], Donald Raoul Tchuifon Tchuifon [a,*], Paul Alain Nanssou Kouteu [a,c], Frank Dorinel Solefack Feudjio [d], Aurelien Bopda [e], Omirserik Baigenzhenov [f,*], Ahmad Hosseini-Bandegharaei [g,h,i,**]

[a] Laboratory of Chemical Engineering and Industrial Bio-Processes (LCEIBP), National Higher Polytechnic School of Douala, University of Douala, P.O. Box 2701, Douala, Cameroon
[b] Institute of Chemistry, Faculty of Process and Systems Engineering, Universität Platz 2, 39106 Magdeburg, Germany
[c] Process Engineering Laboratory, Ucac-Icam Institute, P.O Box 5504, Douala, Cameroon
[d] Laboratory of Applied Physical and Analytical Chemistry, Department of inorganic Chemistry, Faculty of Science, University of Yaoundé 1, PO Box 812, Yaoundé, Cameroon
[e] Advanced School of Mines Processing and Energy Resources, University of Bertoua, P.O. Box 416, Bertoua, Cameroon
[f] Department of Metallurgical Engineering, Satbayev University, Almaty, Kazakhstan
[g] Faculty of Chemistry, Semnan University, Semnan, Iran
[h] Department of Sustainable Engineering, Saveetha School of Engineering, SIMATS, Chennai 602105, Tamil Nadu, India
[i] Research and Innovation Cell, Rayat Bahra University, Mohali, Punjab, India

ARTICLE INFO

Keywords:
Al-Fum MOF
Adsorption
Indigo Carmine (IC)
Orange II (OII)
Optimization

ABSTRACT

This study aims to synthesize and characterize a fumarate-Al-based Metal-Organic Framework (Al-Fum MOF) to evaluate its adsorption properties towards two organic dyes, namely: Indigo Carmine (IC) and Orange II (OII). The Al-Fum MOF was synthesized by a non-solvothermal method and characterized by XRD, FTIR, EDX, TGA, N_2 sorption and pH_{PZC}. The results of this work show that the pseudo-second-order model better describes the adsorption process for both dyes. The plausible mechanisms reveal a duality between the physisorption phenomenon and physicochemical interactions, the latter being predominant. The optimal conditions for adsorption were determined using centered composite experimental designs, resulting in error percentages below 2 %: for IC (pH 3, concentration of 84.7 mg/L and adsorbent mass of 25 mg) and for OII (pH 3, concentration of 100 mg/L and adsorbent mass of 25 g). The adsorbed amounts were 33.8 and 22.9 mg/g for IC and OII, respectively. The regeneration of Al-Fum MOF was studied and the results suggest that the material can remain active during several use cycles. This study contributes to the advancement of knowledge on adsorbent materials for wastewater treatment and highlights the potential of Al-Fum MOF for practical applications. However, further studies are needed to evaluate the application of Al-Fum MOF to real and complex wastewater.

List of abbreviations

Al-Fum MOF	Fumarate-Aluminium-Metal Organic Framworkers
ANOVA	Analysis of Variance
ARE	Average Relative Error
BDC	1,4-benzene dicarboxylic acid
BET	Brunauer-Emmett-Teller
BTC	1,3,5-benzene tricarboxylic acid
Cal.	Calculated
IC	Indigo Carmine
DMF	N,N-dimethylformamide
DTA	Differential Thermal Analysis
EDX	Energy Dispersive X-ray
Exp.	Experimental
FTIR	Fourier Transform Infrared
HYBRID	Hybrid Fractional Error Function

* Corresponding authors.
** Corresponding author at: Faculty of Chemistry, Semnan University, Semnan, Iran.
E-mail addresses: tchuifondonald@yahoo.fr (D.R.T. Tchuifon), o.baigenzhenov@satbayev.university (O. Baigenzhenov), ahoseinib@semnan.ac.ir, ahoseinib@yahoo.com (A. Hosseini-Bandegharaei).

https://doi.org/10.1016/j.rineng.2025.106412
Received 27 April 2025; Received in revised form 11 July 2025; Accepted 21 July 2025
Available online 22 July 2025
2590-1230/© 2025 The Author(s). Published by Elsevier B.V. This is an open access article under the CC BY license (http://creativecommons.org/licenses/by/4.0/).

MOF	Metal-Organic Framework
OII	Orange II
pH	Potential of Hydrogen
pH_{PZC}	pH value at the Point of Zero Charge
RMSE	Residual Mean Squared Error
rpm	Revolution per minute
SEM	Scanning Electron Microscopy
TGA	Thermogravimetric Analysis
XRD	X-Ray Diffraction
χ^2	Chi-Square

1. Introduction

The environmental degradation has reached a critical threshold, compromising the integrity of ecosystems at global scale. This alarming phenomenon results mainly human action, notably urbanization and rapid demographic growth, as well as intensive industrialization [1]. The latter generates considerable flows of toxic substances, frequently rejected in the form of effluents. These pollutants include among others heavy metals [2], pesticides [3], pharmaceuticals products [4] and dyes [5]. The presence of synthetic dyes in water represents a double danger, both for human health and the environment. Indeed, these polluting substances contaminate aquatic ecosystems and can turn out toxic to aquatic organisms, which can enter the eating chain [6]. Among these dyes, indigo carmine and orange II have revealed particular worries because of their toxicity proven, emphasizing thus the necessity of rigorous monitoring and management of these substances. For example, it has been reported that indigo carmine can provoke different pathologies, like hypotension, hypertension, skin irritation or gastrointestinal disorders [7]. Furthermore, the toxic effects of Orange II are manifested by an alteration of hepatic lipid peroxidation and a reduction of red blood cells, hemoglobin and cell volume [8]. Considering the risks posed by these two dyes and their water solubility [9,10], which complicates their elimination, application of specific and efficient treatment methods turns out imperative. Although various techniques are recognized for the decolorization of effluents, adsorption is distinguished as a strategy promising for mitigating environmental pollution caused by these dyes [5,11,12].

The particularity of the sorption process in treatment of water contaminated by pollutants lies in its efficient and economic energy, the absence of generation of secondary pollutants and the possibility to use easily recoverable adsorbents materials, often by simple filtration techniques, which facilitates implementation of the process [11,13]. In addition, the diversity of available adsorbent materials confers on this method a large accessibility and an adaptability to a wide range of pollutants [14–19]. Among these materials, metallo-organic structures constitute a unique material class because of their exceptional property. Indeed, these porous coordination polymers, are distinguished by their raised specific surface area and their porosity adjustable and the presence of unsaturated coordination sites or accessible centers metallic, which give these materials an increased reactivity, thus promoting interactions with species targets [20,21]. Moreover, unlike other adsorbents like zeolites their synthesis is simpler and more practical [21]. The use of MOFs as adsorbent has widely reported these latest years. This is the case of MOFs based on aluminum fumarate which are frequently applied to the capture of ions in aqueous solution. As illustrative, Karmaka et al. [22], have synthesized an aluminum fumarate - based MOF for fluoride removal in aqueous solution. Their results have revealed an adsorption ability very high maximum of 600 mg/g at 293 K. In the same wake, Moumen et al. applied an aluminum fumarate-based MOF on the removal of phosphate in aqueous media [23]. This material demonstrated good adsorption properties, with an adsorption ability of 67.62 mg/g, surpassing those obtained in using aluminum- based MOFs, synthesized from organic ligand derivatives of petroleum sources such as BTC (1,3,5-benzene tricarboxylic acid) and BDC (1,4-benzene dicarboxylic acid). This work sufficiently illustrates the good adsorbent property of aluminum fumarate MOFs. The aluminum fumarate-based MOF has a crystalline structure similar to that of the MIL-53 and an excellent stability in water. It is an accessible material at low cost, which also offers the advantage of being non- toxic. In fact, the fumaric acid used as ligand is one of the least expensive and less toxic that can be used in the synthesis of MOFs [22,23].

In this context, the present study explores the synthesis and application of a fumarate-based aluminum metal-organic framework as a novel adsorbent for the removal of two industrially significant dyes, Indigo Carmine and Orange II, from aqueous solutions. Although Al-Fum MOF is known for its water stability, porosity, and low toxicity, its adsorption capacity for these specific dyes has not yet been thoroughly investigated. The originality of this work lies in its dual focus: first, on optimizing the adsorption process using a response surface methodology based on a centered composite design, and second, on elucidating the adsorption mechanisms through comprehensive kinetic and isothermal modeling, including pseudo-first-order, pseudo-second-order, Elovich, intraparticle diffusion, Langmuir, Freundlich, Temkin, and Dubinin–Radushkevich models. Furthermore, this study evaluates the regeneration and reusability of the Al-Fum MOF, thereby highlighting its potential for repeated use in practical wastewater treatment scenarios. By addressing a gap in current research and offering a low-cost, effective, and environmentally sustainable solution for dye removal, this work contributes meaningful insights toward the development of next-generation adsorbent materials for industrial effluent treatment.

2. Materials and methods

2.1. Materials and reagents

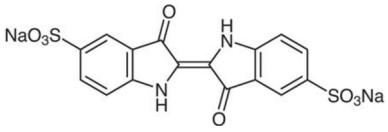
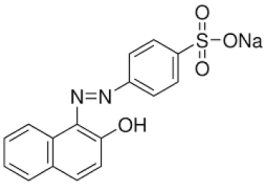
The exploited chemicals in the current study are of analytical grade. Indigo Carmine and Orange II (characteristics are given in Table 1) are pollutants from Sigma Aldrich, except for all other reagents from the international company *Fisher scientific*. Fumaric acid (C_4 H_4O_4; 98 %) and aluminum sulfate hydrate ($Al_2(SO_4)_3{\cdot}18H_2O$; 98 %) obtained from Prolabo chemical industries, were exploited as organic ligand source and metal source respectively for the synthesis of Al-Fum MOF. Sodium hydroxide (NaOH; 99.5 %) and nitric acid (HNO_3; d = 1.18) were obtained from BDH Chemicals, were exploited to adjust the pH values during the adsorption study. Acetone, ethanol, DMF (N,N-dimethylformamide) were obtained from BDH Chemicals and distilled water were used as solvents.

2.2. Methods

2.2.1. Fumarate- aluminium-metal organic framworkers (Al-Fum MOF) synthesis

The sorbent (Al-Fum MOF) was fabricated based upon a non solvothermal method as described in the literature [24], but with some modifications. In a 50-mL round-bottom flask, a measured combination of aluminum chloride ($AlCl_3$, 0.500 g, 3.74 mmol) and fumaric acid ($C_4H_4O_4$, 0.532 g, 4.62 mmol) was dissolved in 20 mL of DMF. The resulting pale-yellow cloudy suspension was then maintained underneath constant agitation at an elevated temperature of 130 °C for an extended period of 100 hours. When slowly cooled to room temperature, the reaction mixture yielded a white precipitate, which was isolated by slow filtration. The resulting solid was subsequently purified appropriately through successive washes with solvents. The precipitate was initially subjected to two treatments with acetone (200 mL each) for 1 h and 24 h, respectively. Then, the solid was washed with two washes of ethanol (each 200 mL), again for 1 h and 24 h. The final purification was achieved by drying the purified solid at a controlled temperature of 80 °C to get the product. The mass of the final product is 0.830 g, giving a reaction yield of 90 %. The balanced equation of the synthesis is summarized by the following Fig. 1:

Table 1
Characteristics of Indigo Carmine and Orange II.

Indigo Carmine		Orange II
Chemical structure		
Molecular formula	$C_{16}H_8N_2Na_2O_8S_2$	$C_{16}H_{11}N_2NaO_4S$
Nomenclature	[3,3′-dioxo-1,3,1′,3′-tetrahydro-[2,2′]-bi-indolylidene-5,5′- disulfonic acid disodium acid]	4-(2-hydroxy-1-naphthylazo) benzenesulfonic acid sodium acid salt; Sodium4-[(2-hydroxy-1- naphthyl) azobenzenesulfonate]
Molar mass	466.35 g/mol	350.32 g/mol
Color	Dark blue	Orange
Appearance	Powder	Powder

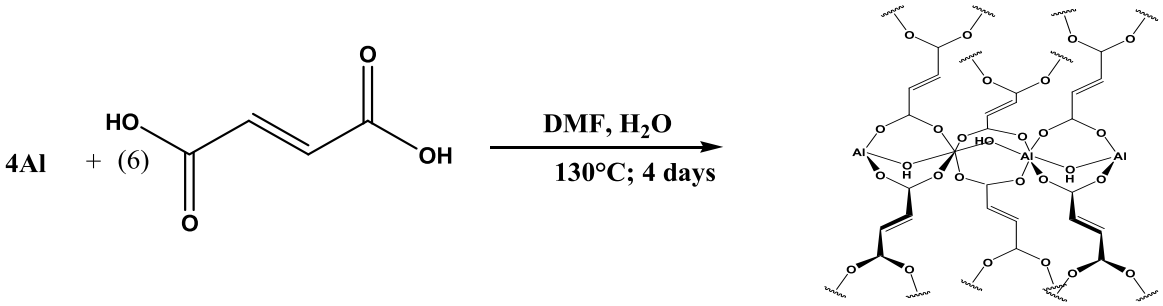


Fig. 1. Balanced reaction for the synthesis of sorbent (Al-Fum MOF).

2.2.2. Characterization of Al- Fum MOF

The Al-Fum MOF produced were analyzed in order to scrutinize the physico-chemical characteristics of this material. Physicochemical material characterization employed a variety of advanced analytical techniques. Analysis of molecular structure and functional groups was conducted by the aid of vibrational spectroscopic analysis via Fourier Transform Infrared (FT-IR) spectroscopy, employing a Nicolet Thermoscientific IS5 spectrophotometer. Surface topography and elemental composition were analyzed by Scanning Electron Microscopy with Energy Dispersive X-ray Analysis (SEM/EDX), performed on a TESCAN VEGA 3-LMU microscope at an accelerating voltage of 8 kV. Specific surface area wes determined by gas adsorption by the Brunauer-Emmett-Teller (BET) method on a BELSORP MAX instrument from Bel Japan Inc. The technique provided critical information regarding the porosity and surface characteristics of the material. The specific surface area, pore size, and pore volume of the materials were determined using N_2 adsorption and desorption isotherms using the BET/BJH models. Prior to the N_2 physisorption experiment, the sample was pre-heated for 1 h at 150 °C and then remaining water vapour and CO_2 molecules were evacuated from the pores of the sample by thermally heating it at 30 °C. Crystallographic analysis was conducted by the use of X-ray diffraction (XRD), which allowed for the detection and quantification of crystalline phases and detection of amorphous material, exploiting a PAN analytical XPERT Pro powder diffractometer automated with anode filtered Cu-$K_{\alpha 1}$ radiation. The TGA and DTA analyses of biomasses (RS and RC) were performed using a differential thermogravimetric analyzer, combining a thermogravimetric analysis on (Mettler Toledo, TGA STAR system), as well as a LECO–701 thermogravimetric analyzer.

2.2.3. Adsorption test on Al-Fum MOF in bacth process: influence of significant parameters

All tests were conducted at room temperature. Indigo Carmine and Orange II were adsorbed on Al-Fum MOF material using the bach process, including different parameters such as the mass of sorbent, the solution's pH, the contact time, and the pollutant concentration in aqueous media. 50 mg of Al-Fum MOF material was used as a fixed amount. However, in investigating trials the effects of Al-Fum MOF dose, the amount of material used change from 25 to 125 mg. 0.01 mol/L HNO_3 or NaOH solutions were exploited to adjust pHs of solutions. The pH span under investigation was 3 to 8. In experimental tests, 50 mg of Al-Fum MOF was mixed with 30 mL of Indigo Carmine or Orange II solution, and the mixture was agitated by stirring at 150 rpm and at time intervals from 5 to 180 min. The Al-Fum MOF was filtered out of the mixture, and the quantities of Indigo Carmine or Orange II in filtrate were determined by exploiting a SECOMAN UV–visible spectrophotometer (SECOMAM, model S 500) at 510 nm for Orange II and 640 nm for Indigo Carmine to determine the residual concentrations. Therefore, Eqs. 1 and 2 were used to determine the quantity of each dye adsorbed (Qads) and its adsorption percentage, R (%):

$$\boldsymbol{Q_{ads}} = \frac{(\boldsymbol{C_0} - \boldsymbol{C_e})\boldsymbol{V}}{\mathbf{m}} \quad (1)$$

$$\mathbf{R} = \frac{\boldsymbol{C_0} - \boldsymbol{C_e}}{\boldsymbol{C_0}} \times 100 \quad (2)$$

where V is the volume of solution (L), C_e is the concentration of the dye at equilibrium (mg/L), C_0 is the dye's starting concentration (mg/L), and m is the sorbent's mass (mg).

2.2.4. Theoretical foundations of modeling

To elucidate the governing mechanisms of the adsorption, the kinetic data were analyzed comprehensively based on four kinetic models presented in Table 1, for both Indigo Carmine and Orange II onto the Al-Fum MOF. The entire procedure enabled a refined understanding of the process of adsorption such that determinants controlling it could be established. The exploitation of different kinetic models serves to unveil

intricate dynamics of adsorption process, giving information on various aspects such as reaction order, rate-controlling steps, and potential diffusion mechanisms. Through the use of the experimental data within these different mathematical models, we can determine the model that best explains the resulting kinetic behavior, hence gaining insight into the involved physicochemical processes not only further enhances our knowledge of the adsorption kinetics but also forms a solid foundation for the optimization of the adsorption process in practical applications. This comparative examination gives a more nuanced insight into the adsorption mechanisms, possibly revealing nuances that might otherwise get lost due to the nature of an isolated model approach. Table 2 summarize the applied different models.

The adsorption equilibrium aspects of Indigo Carmine and Orange II adsorption onto the Al-Fum MOF were also comprehensively studied with rigorous application of two-parameter non-linear isotherm models (Table 3), which enabled the elucidation of underlying adsorption mechanisms and surface interactions. The technique employed high-level regression techniques to optimize model parameters, systematically varying both adsorption capacity (Q_e) and affinity constants and adjusting for non-uniform error distributions in linearized transformations.

2.2.5. Quality of fit

The "goodness of fit" test quantifies how closely a curve matches experimental data. This may be aided by quantities such as the coefficient of determination, R^2, which quantify proportion of variation in one variable that can be accounted for by another. Although R^2 can be used for nonlinear models like isothermal equations, it does not include errors in the curves automatically. In order to overcome this limitation, some nonlinear error functions are exploited to determine the correctness of fit of the equilibrium models. They include the average relative error (ARE), the hybrid fractional error function (HYBRID), the Chi-Square (χ^2) test error function [33], and the residual mean squared error (RMSE) (Table 4). Each of these functions provides another method for evaluating model fit through measuring discrepancies between observed and predicted values, giving a summary measure of model performance [34].

2.2.6. Optimization: response surface design (central composite design 2^3 +star)

Response surface methodology, a set of mathematical and statistical techniques, offers a strong framework for modeling and investigating complex systems where a response variable is influenced by interactions among numerous factors [35]. In the present study, a 23 + star centered composite design, being a standard response surface methodology design, was exploited to assess synergistic interaction of various parameters in Indigo Carmine and Orange II adsorption using Al-Fum MOF with the ultimate goal of identifying optimal conditions of the adsorption process. This method enables more effective understanding of the interactions of the variables with the response to enable optimization of the adsorption process. In the current work, the variables exploited are (i) the concentration of the pollutant (X_1); (ii) the mass of the adsorbent (X_2) and (iii) the pH of the pollutant solution (X_3). The range and levels of the variables are demonstrated in Table 5. The responses are the sorbed amounts (Y_1) and the adsorption percentage (Y_2).

Table 2
Nonlinear equations for kinetic models.

Kinetic	Non-linear form	Reference
PFO (Pseudo-first order)	$Q = Qe\left(1 - e^{-K_1.t}\right)$	[25]
PSO (Pseudo-second order)	$Qt = \frac{Qe^2.K_2.t}{1 + Qe.K_2.t}$	[26]
Elovich	$Qt = \frac{1}{\beta}\ln(\alpha\beta) + \frac{1}{\beta}ln(t)$	[27]
Intraparticle diffusion (ID)	$Qt = K_d(t)^{1/2} + C$	[28]

Table 3
Nonlinear forms of two-parameter isothermal adsorption models.

Isotherm	Non-linear form	Reference
Langmuir	$Qe = \frac{Qm\ KCe}{1 + KCe}$	[29]
Freundlich	$Qe = K_F\ Ce^{\frac{1}{N}}$	[30]
Temkin	$Qe = Qm\frac{R}{\Delta Q}ln(K_T Ce)$	[31]
Dubinin Radushkevick	$Qe = Qm.e^{-K\varepsilon^2}$	[32]

Table 4
Expression of different error functions of nonlinear forms.

Functions of errors	Formulas
R^2	$1 - \frac{\sum_{i=1}^{n}(Qe,\exp - Qe,\ cal)^2}{\sum_{i=1}^{n}(Qe,\exp - \overline{Qe,\ cal})^2}$
X^2	$\frac{\sum_{i=1}^{n}(Qe,\exp - Qe,\ cal)^2}{(Qe,cal)^2}$
RMSE	$\sqrt{\frac{1}{n-2}\sum_{i=1}^{n}(Qe,\exp - Qe,\ cal)^2}$
HYBRID	$\frac{\frac{100}{n}\sum_{i=1}^{n}(Qe,\exp - Qe,\ cal)^2}{Qe,exp}$
ARE	$\frac{100}{n}\sum_{i=1}^{n}\frac{\lvert Qe,\mathrm{cal} - Qe,\ exp)\rvert}{Qe,exp}$

Table 5
Levels of variables.

Variables	Minimum value (-1)	Value in the center (0)	Maximum value (+1)
Pollutant concentration (X_1) in mg/L	20	60	100
Mass (X_2) in mg	25	75	125
pH (X_3)	3	5.5	8

An empirical model was formulated on the basis of a second-degree polynomial to establish a parameter-target response correlation, mathematically as given by Eq. 3. The approach utilizes a quadratic expression for global fitting and characterizing an independent variable (parameter)-dependent variable (target response) relationship. Utilization of a second-degree polynomial offers a good balance between model simplicity and accuracy, characterizing the inherent relationship without unnecessary complication:

$$\boldsymbol{Y} = \boldsymbol{b}_0 + \sum_{i-1}^{n}\boldsymbol{b}_{ii}\boldsymbol{x}_i + \left(\sum_{i-1}^{n}\boldsymbol{b}_{ii}\boldsymbol{x}_i\right)^2 + \sum_{i-1}^{n-1}\sum_{j-i+1}^{n}\boldsymbol{b}_{ij}\boldsymbol{x}_j \quad (3)$$

where he anticipated response is denoted by Y, the interaction coefficients by b_{ij}, the constant and quadratic coefficients by b_0, and coded values of the interaction variables by x_i and x_j.

The statistical software *Statgraphics 18* was exploited to analyze the data of experimental design. ANOVA (Analysis of variance) and regression analyses were done to fit developed equations.

The total number of experiments (N) in a central composite design can be elegantly expressed as a function of the number of factors (n) and center points. This sophisticated formulation is represented by the equation [36]:

$$\boldsymbol{N} = 2^n + 2\boldsymbol{n} + \boldsymbol{n}_{centre} = 2^3 + 2{*}3 + 6 = 20 \quad (4)$$

This equation consists of 2^4 factorial points, 2*4 axial points, and 6 centers points. Data reproducibility and experimental error were assessed using the center points.

2.2.7. Regeneration: washing and moderate heat treatment

The ability of Al-Fum MOF to maintain its efficiency over five

adsorption cycles was evaluated. The first cycle was performed using 100 mg of Al-Fum MOF in 50 mL of dye solution at the optimal concentration and pH. Stirring was maintained for up to 150 min, after which the mixture was filtered and analyzed by UV–visible spectrophotometry. The percentage of dye adsorption in this first cycle was calculated from Eq. 2. The Al-Fum MOF material was recovered from the solution after this first cycle by filtration. The recovered material was washed with deionized water by centrifugation three times at 3000 rpm for 5 min. After washing, the material was dried in an oven at 100 °C for 2 h and used in the next adsorption experiment. Three further tests were carried out to obtain results for five consecutive cycles of experimental tests and the corresponding percentages of dye adsorption were calculated.

3. Results and discussion

3.1. Characterization of Al-Fum MOF

3.1.1 X-ray diffraction (XRD), Fourier Transform Infrared (FTIR), Scanning electron microscope (SEM) and Thermogravimetric analysis of Al-Fum MOF

The results of XRD analysis of Al-Fm MOF are reported in Fig. 2a.

This spectrum shows a first intense peak at 2θ =10.6°, with other small peaks of low intensity at successive 2θ values of 14.97; 22.17; 31.80 and 43.23° All these peaks would correspond respectively to the intensity of the presence of the Al^{3+} ion according to its distribution within the structure of the material [37]. These ions are therefore at the center of the Al-O clusters, which in turn are linked to organic ligands (fumaric acid) to form the structure of the Al-fum MOF. The structure of the MOF is therefore easily considered stable and pure with the absence of additional peaks in this spectrum. All these investigations are in line with those of Al-fum MOF synthesized by Wei et al., in 2017, during their work on the experimental evaluation of the isotherms and the kinetics of sorption of water on aluminum fumarate [38]. The size of Al-fum MOF calculated by Scherrer formula gives D ≈ 17.8 nm which indicates that the crystallites of Al-fum MOF have a nanometric size. This size is relatively small, which may have importantes implications for the properties and applications of the material [39].

Analysis of this spectrum (Fig. 2b) reveals the presence of numerous adsorption bands that confirm the existense of the characteristic functional moieties in the material. It presents an adsorption band around 596 cm^{-1} characteristics of the Al-OH bond [40]. This bond would therefore be established between the aluminum atom coming from aluminum sulfate and water molecules. It also shows 1615 and 1424 cm^{-1} bands attributable to stretching (asymmetric and symmetric respectively) of fumarate's carboxylic moieties [41]. All this information argues in favor of the Al-Fum MOF in analogy with that synthesized by Moumen et al in 2022 [41], and confirms the success of the synthesis.

The SEM image, displayed in Fig. 2c, is used to assess the morphology and particle size of the manufactured Al-Fum MOF powders. These Al-Fum particles are quadrilateral in form, ranging in size from 60 to 100 nm. Particles are shown to be strongly agglomerated. According to reports, metal carboxylates are incredibly stable to water, making them an excellent choice for water adsorption. Al-Fum MOF is therefore expected to be a sensible option for adsorption.

The evolution of the physical and chemical characteristics of the Al-

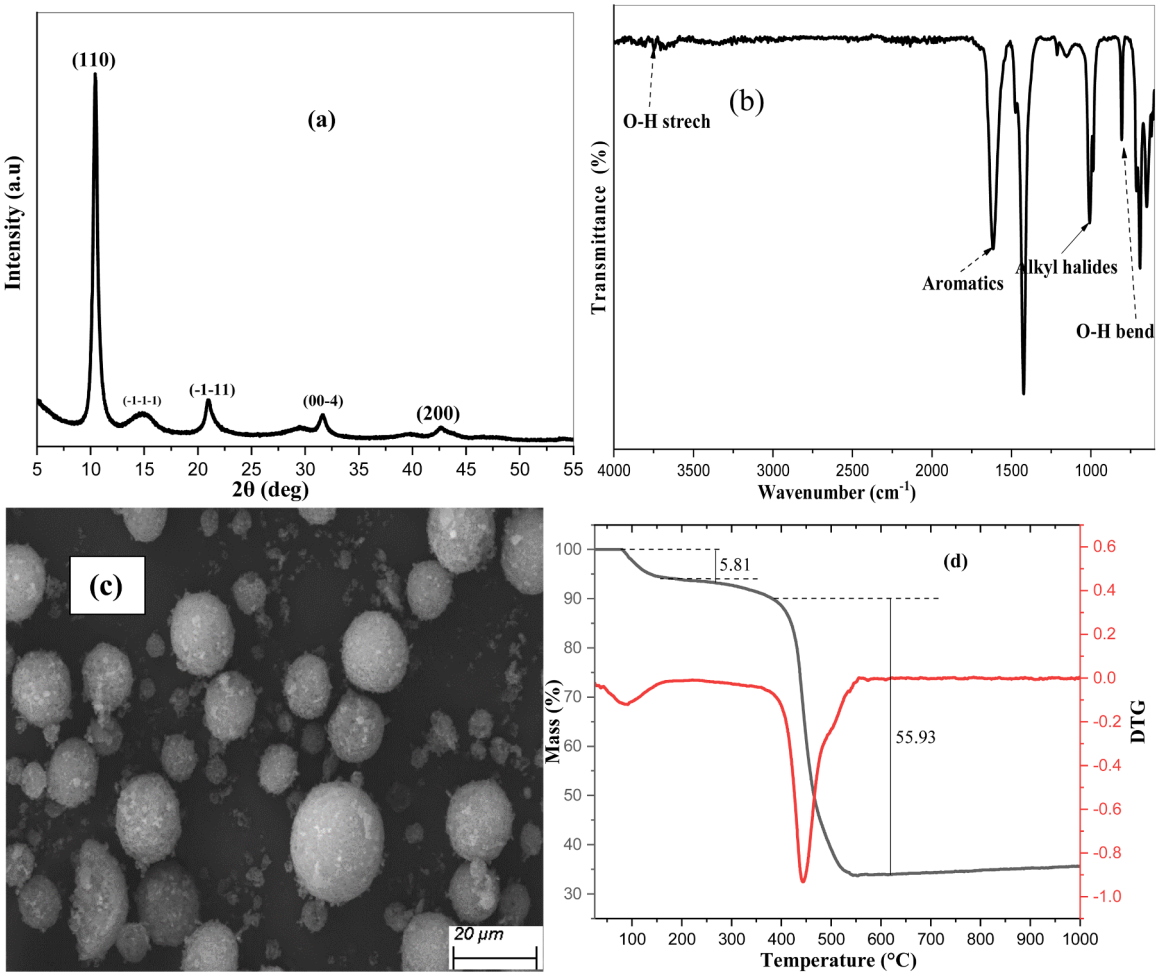


Fig. 2. XRD pattern (a), FTIR (b), SEM images (c) and TGA (d) analyses of Al-Fum MOF.

Fum MOF as a function of temperature is illustrated in Fig. 2d It can be grasped that degradation occurs in two stages. The first represents the adsorbed moisture vaporizing at 90 °C and the second stage is the thermal degradation of the material at 445 °C.

Fig. 3 in its part (a) presents the results of elemental content of the Al-Fum MOF which was determined by energy dispersive X-ray spectroscopy. It appears that presence of aluminum is evaluated at (8.7 %), that of oxygen at (33.6 %) and that of carbon at (57.7 %). These percentages are in line with those of Karmakar et al. [22]; this which would allow us to confirm that it is the Al-Fum MOF. In its part (b) it also presents a cartographic portion which also confirms the presence of aluminum, oxygen and carbon elements respectively in proportions of 40, 21 and 39 %. All this cumulative information indicates that the molecular structure of our material is mainly made up of carbon and oxygen coming from the organic ligand: fumaric acid (trans-butene-1,4-dicarboxylic acid: HO_2C-CH=CH-CO_2H) and also of aluminum representing the central metal of the molecular structure coming from aluminum chloride.

The adsorption-desorption isotherm of Al-Fum MOF obtained is presented in the following Fig. 4 and Table 6.

The curve in Fig. 4 of the Al-Fum MOF exhibits a type IV physisorption isotherm implying that this adsorbent is mesoporous. BET results show that the Al-fum MOF has a high specific surface area and a large pore volume (Table 6), which is characteristic of porous materials. The average pore diameter is relatively small, suggesting that the pores are mainly micropores or mesopores. According to Ferey (2008) [42], MOFs (Metal–Organic Frameworks) are porous materials that exhibit unique properties, such as high specific surface areas and large pore volumes. These properties make them attractive for applications such as gas storage, gas separation, and catalysis. The high specific surface area of the Al-Fum MOF is comparable to those of other MOFs reported in the literature. For example, the MIL-53(Al) MOF has a specific surface area of 1140 m^2/g [43]. The average pore diameter of the Al-Fum MOF is relatively small, which is consistent with the structure of MOFs. According to Rowsell and Yaghi [43], MOFs can have pores of various sizes, ranging from a few angstroms to several nanometers. The results obtained for the Al-Fum MOF show that this material has a high specific surface area and a large pore volume, which is characteristic of MOFs. The average pore diameter is relatively small, which suggests that the pores are mainly micropores or mesopores.

The pH_{PZC} value of the material is obtained by determining intersection point betwixt the curve ΔpH= f(pHi) and horizontal line passing through the origin as shown in the following Fig. 5. It appears that the pH value at the point of zero charge (pH_{PZC}) of the synthesized Al-Fum MOF is 4.82 (less than 7), which implies that the latter has acidic functional groups at its surface (carboxylic functional groups from fumaric acid). Indeed, when the pH of the solution is lower than the pH_{PZC}, the surface of the adsorbent will predominantly be positively charged and the adsorption will therefore be maximum for negatively charged adsorbates. If the pH of the solution is greater than the pH_{PZC}, the surface of the adsorbent will predominantly be negatively charged; the adsorption will be maximum with negatively charged adsorbates [44]. It is therefore possible to predict maximum adsorption for the anionic pollutants of our study in an acidic pH range (less than 4.82). However, the affinity will be much greater with Indigo Carmine which has two characteristics negatively charged sites (-SO_3^-), compared to Orange II which has only one.

3.2. Adsorption test on Al-Fum MOF: influence of significant parameters

The parameters affecting adsorption studied in this work are: pH, contact time, mass of Al-Fum MOF used, initial concentrations of Orange II and Indigo Carmine.

3.2.1. Influence of pH

The influence of pH on adsorption capacity of Orange II and Indigo Carmine by Al-Fum MOF was scrutinized by varying the pH of the solutions of different pollutants from 2 to 8. The effects during these tests are shown in Fig. 6a. The coupled histogram in Fig. 6a vouchsafes that MOF Al- Fum exhibits good adsorption performances for Indigo Carmine and Orange II over a pH range of 3 to 8. However, the removal

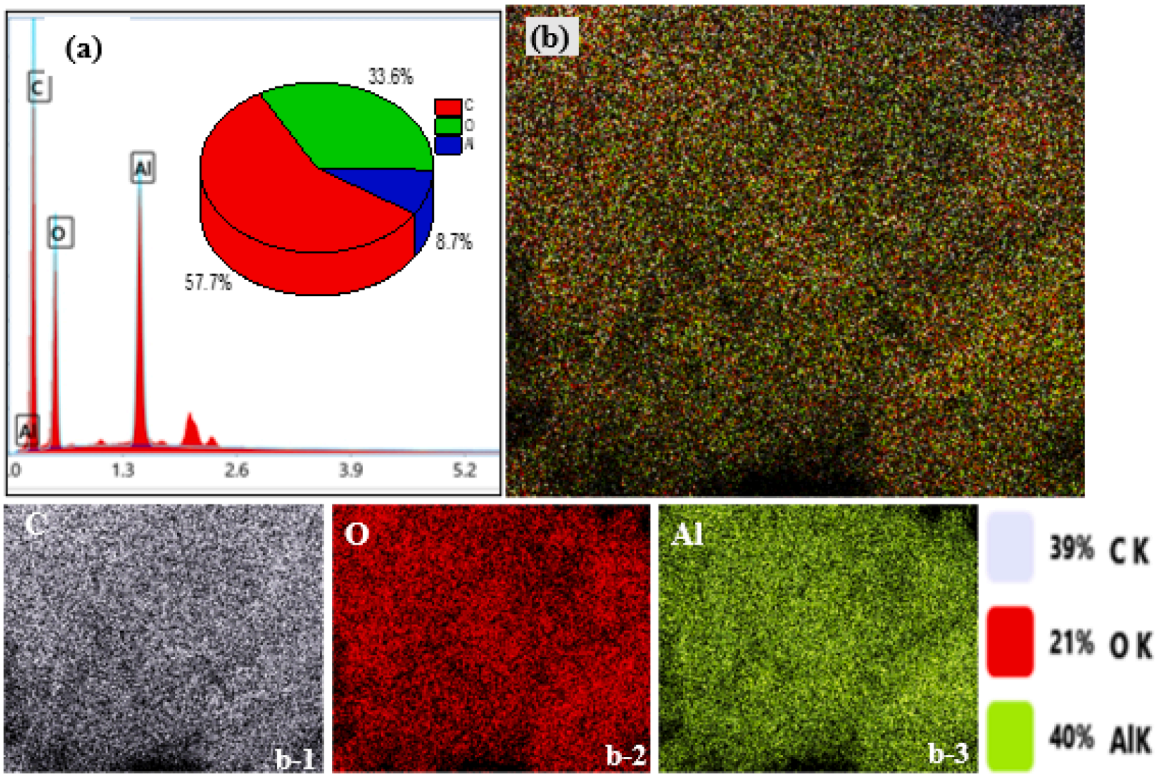


Fig. 3. EDX elemental compositions (a), EDX mapping (b) and distribution mapping of C, O and Al elements (from b1 to b3 respectively).

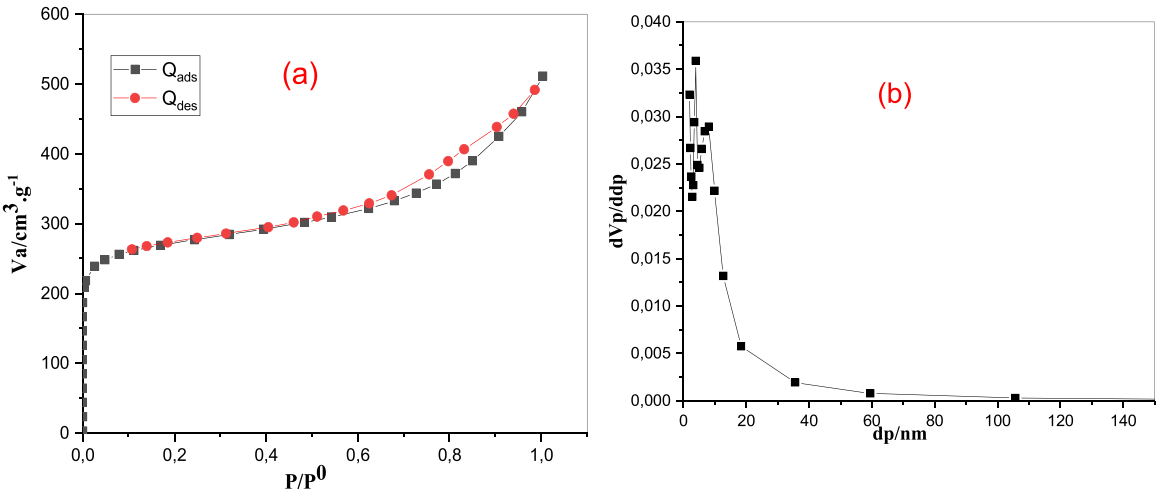


Fig. 4. BET isotherm (a) and pore size distribution (b) of Al-Fum MOF.

Table 6
Specific surface area values of Al-Fum MOF.

	Al- Fum MOF
Pore volume (cm^3/g)	0.4702
Specific surface area (m^2/g)	1025.3
Average pore diameter (nm)	1.8344

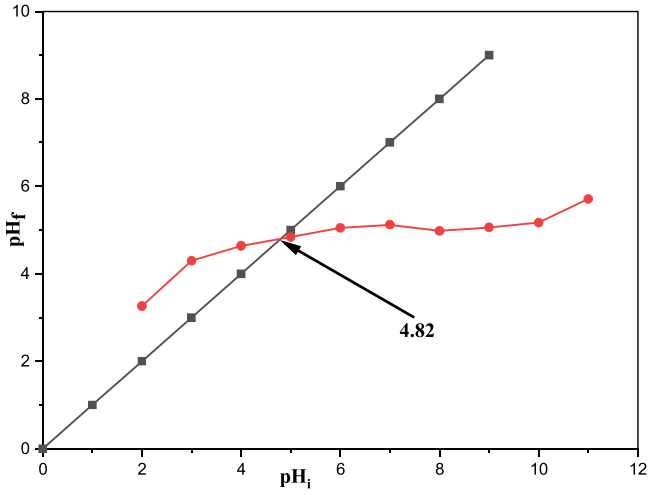


Fig. 5. pH at the zero charge point of the Al-Fum MOF.

performances are significantly better for Indigo Carmine compared to those of Orange II. The results clearly prove that highest adsorbed amounts of the different dyes are produced at acidic pH. The maximum adsorbed amounts for Orange II and Indigo Carmine are noted at pH = 3 and pH = 4, respectively, with respective values of 13.3 and 24.1 mg/g. These results would indicate that the pollutants would be primarily adsorbed on the Al-fum MOF by electrostatic interactions, because for these pH values lower than the pH_{PZC}, the adsorbent material is positively charged while the pollutants are anionic in aqueous solution due to their molecular structures. However, the difference between these two values would be justified by the fact that the Indigo Carmine contains more negatively charged sites (2 SO_3^- groups) than the Orange II (1 SO_3^- group). Moreover, when the pH approaches 4.82 (pH_{PZC}) and/or tends towards 8, the removal efficiency of the latter declines owing to electrostatic repulsions betwixt anionic dyes and negative surface of the material. Such outcomes are in agreement with those of Karmaka et al. in 2016 [22] on the removal of fluorine by the Al- Fum MOF. Furthermore, at low pH, nucleophilic substitution of the "OH^- "group by the "-SO_3^- " group would be easy and we would then witness a ligand exchange on the metal ion Al^{3+} which would confirm a physiochemical phenomenon between the material and the different pollutants. Moreover, at higher pH and owing to the abundance of OH^-, this type of nucleophilic replacement is not favored.

3.2.2. *Influence of contact time*

The results obtained were illustrated in Fig. 6b, the first stage is observed during the first 5 min, where an exponential and rapid adsorption takes place. These strong adsorptions would be mainly linked to meso-sized pores generated by the agglomeration of the Al-Fum MOF particles, to the considerable number of metallic sites and also to the large contact surface [42]. Then, in the second stage, in which the adsorptions are more moderate, slow and last approximately 55 min for Indigo Carmine and 75 min for Orange II; these regressions would result from a reduction of the adsorption surface sites, the molecules of the different pollutants are therefore forced to migrate progressively towards more internal adsorption sites and low surface areas to be able to attach to the material. After respectively 60 and 80 min of contact for Indigo Carmine and Orange II, a very small variation in the adsorbed quantities of the pollutants by the material is observed; are around 25.3 mg/g for Indigo Carmine and around 12.5 mg/g for Orange II. This phenomenon characterizes the third stage where it would be assumed that all the adsorption sites present on the material would be occupied or saturated, consequently a simultaneous adsorption/desorption phenomenon would happen on surface of material while maintaining the sorbed quantities almost fixed.

3.2.3. *Influence of mass*

The effect of the adsorbent dosage (Al-Fum MOF) in this study is determined at optimal pH and time conditions, and at an initial concentration of 100 mg/L for each of pollutants. The results obtained are recorded in Fig. 6c. The adsorbed quantities decrease considerably with the increase in the mass of the adsorbent because of the decrease in the total available surface area caused by the aggregation and congestion of the adsorption sites. A continuous increase in mass would lead at a given time to an agglomeration or cluster of cells which could lead to a reduction in intercellular distances [45]; which would produce a screening effect leading to the protection of the binding sites of the anionic molecules of the pollutants. The removal efficiency of both pollutants increases with the augmentation in adsorbent dosage from 25 mg to 125 mg. The elimination percentage increases to 72.7 % for Indigo Carmine and to 58.5 % for Orange II. This observation can be explained

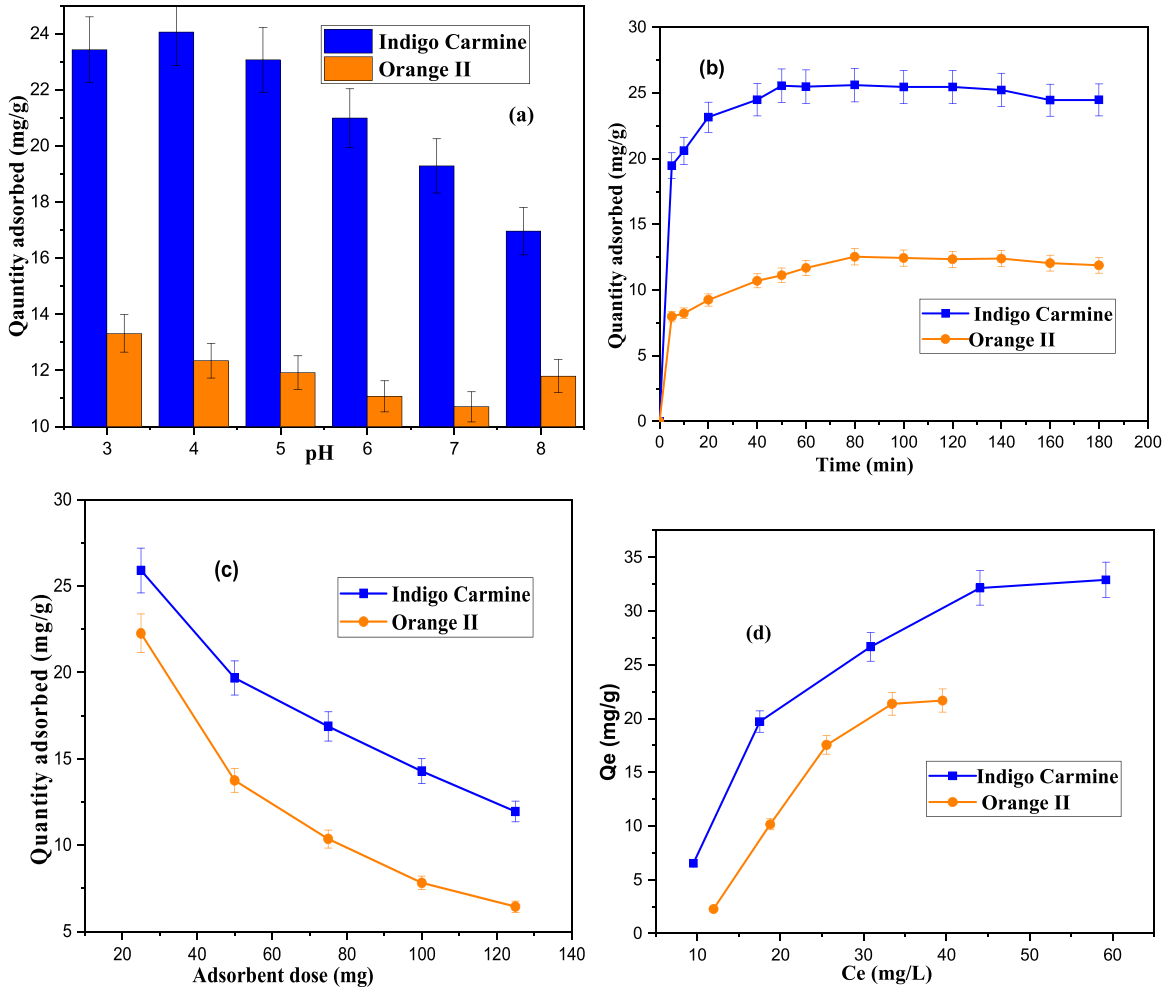


Fig. 6. Influence of significant parameters: (a) pH, (b) contact time, (c) mass of the sorbent and (d) concentration of the pollutant.

by the fact that augmentation in mass of the adsorbent gives rise to an augmentation in specific surface area and therefore the number of available active sites [41].

3.2.4. *Influence of the initial concentration of the adsorbate*

The influence of the initial concentration is scrutinized by varying initial concentrations of solutions. Shapes of the different curves obtained by plotting $\boldsymbol{Qe} = \boldsymbol{f}(\boldsymbol{Ce})$ are shown in Fig. 6d. It is generally observed that the adsorbed quantities of the two pollutants increase with the initial concentration, which can be assigned to availability of a large number of adsorption sites for low concentration values [41]. This increase could also be elucidated by presence of a large number of molecules that will diffuse towards the surface of sorbent when the initial concentration is high and therefore the retention becomes more important. Indeed, the augmentation in concentration leads to the creation of a significant transfer force of the pollutant molecules to the surface of the adsorbent as explained by Fick's first law on mass transfer when it states that: "during the transfer of matter by the diffusion phenomenon, it moves from the most concentrated medium to the least concentrated medium in order to establish a uniform distribution across a surface and the flow of matter is proportional to the concentration gradient". The quantity of molecules present on this surface increases and therefore promotes adsorption [46].

3.3. *Modeling of adsorption kinetics*

To describe sorption dynamics of Indigo Carmine and Orange II onto Al-Fum MOF, the non-linear pseudo-first; pseudo-second order; intra-particle and Elovich models were studied by plotting the curves $\boldsymbol{Qt}$ as a function of time ($\boldsymbol{Qt} = \boldsymbol{f}(\boldsymbol{t})$) shown in Fig. 7a and b respectively for adsorptions of both dyes (Indigo Carmine and Orange II). The corresponding kinetic parameters were recorded in Table 7.

Outcomes reported in Table 7 demonstrate that coefficients of determination (R^2) of pseudo-first order and pseudo-second order models for the adsorption of the two dyes are nearly 1.0. The nonlinear models therefore demonstrate that the mechanisms governing these adsorptions would be governed by chemical interactions. This parameter is not only close to 1 but also betwixt 0.805 and 0.983 for the Elovich model, which confirms that it would be a physiochemical process between the active sites of the material surface and the different ionic solutions [39]. Based upon the low amounts of χ^2 as well as those of their RSME and HYBRID error functions, these same models better describe the adsorptions of the two pollutants on the Al-Fum MOF. Moreover, all these values are lower and therefore favorable for a pseudo-second order model. Other researchers such as Moumen et al [41]., have shown following their work that the pseudo-second order model was also the best fitted one for sorption of phosphorus on Al-Fum MOF. The pseudo-second order kinetic model highlights the chemical interactions betwixt the adsorbate and the adsorbent [47]. It reveals that sorption rates of Indigo Carmine and Orange II on Al-Fum MOF would depend on the nature of the active sites available on material and concentrations of different pollutants in aqueous media as shown above through the influence of the parameters governing the phenomenon. The adsorption would then be monolayer, so physiochemical interctions

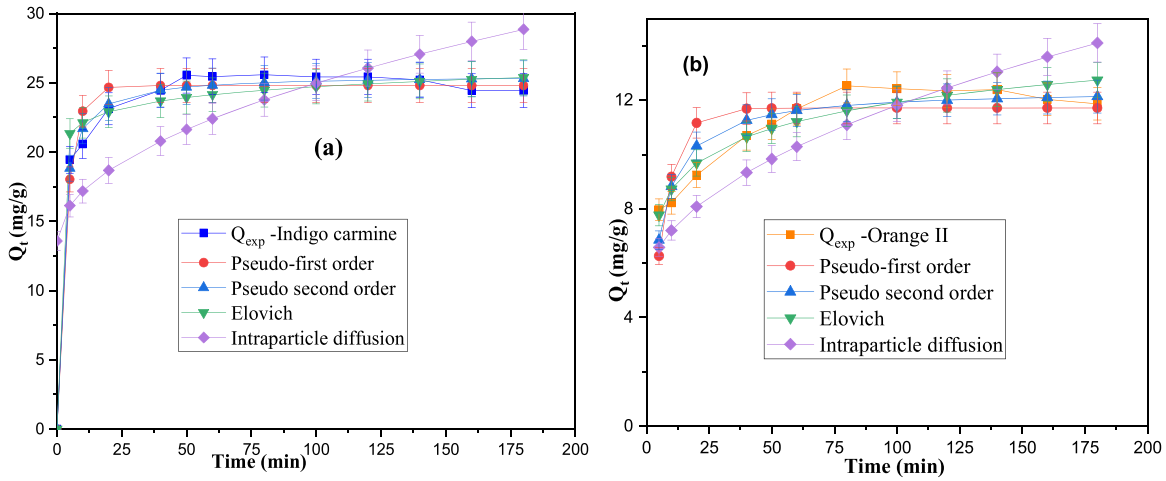


Fig. 7. Non-linear kinetic models plot of Indigo Carmine (a) and Orange II (b).

Table 7
Kinetic parameters of Al-Fum MOF on Indigo Carmine and Orange II.

No.	Models	Constants	Values	R^2	RSME	χ^2	HYBRID	ARE	EABS
Indigo Carmine									
1	**PFO**	Q_e (mg/g)	24.816	0.978	3.592	0.564	11.878	5.591	8.784
		K_1 (min^{-1})	0.259						
2	**PSO**	Q_e (mg/g)	25.571	0.992	2.191	0.175	4.145	1.118	1.800
		K_2 (g/min.mg)	0.022						
3	**Elovich**	α (mg/ g.min)	369	0.940	3.792	0.586	12.670	4.585	7.337
		β (g /mg)	0.886						
4	**ID**	K_p (mg/g.$min^{0.5}$)	1.140	0.001	17.449	18.507	102.010	64.381	137.938
		C (mg/g)	13.586						
Orange II									
1	**PFO**	Q_e (mg/g)	11.714	0.923	3.315	1.143	23.444	36.897	24.863
		K_1 (min^{-1})	0.153						
2	**PSO**	Q_e (mg/g)	12.406	0.970	2.071	0.451	9.086	14.904	10.044
		K_2 (g/min.mg)	0.020						
3	**Elovich**	α (mg/ g.min)	74.097	0.920	1.704	0.171	5.121	5.287	3.633
		β (g /mg)	0.720						
4	**ID**	K_p (mg/g.$min^{0.5}$)	0.674	0.529	6.767	6.445	37.150	101.693	91.871
		C (mg/g)	5.070						

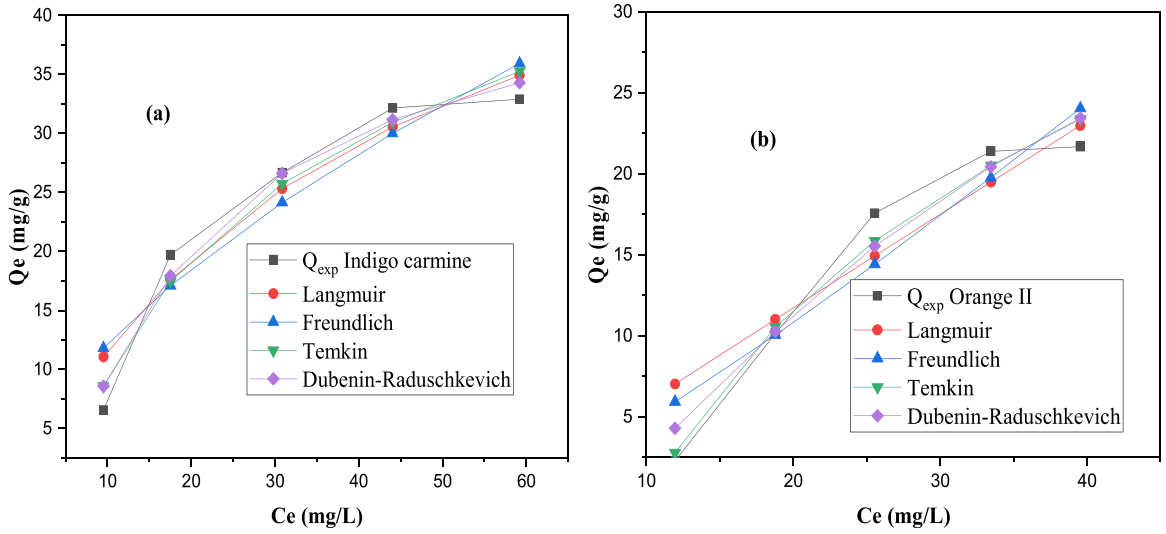


Fig. 8. Non-linear modeling of fixed-time isotherms of Indigo Carmine (a) and Orange II (b).

would dominate the adsorption processes of this study. The low values of the external diffusion constant k_{id}, as well as those of its R^2 obtained, show that intra-particle diffusion is a significant step in these adsorption processes, especially after the first 5 min as observed during the influence of the contact time. This latency time could be explained by the movement of dye molecules in the pore channels of the adsorbents, before reaching the surface where they will be fixed.

3.3.1. Modeling of fixed-time isotherms

Adsorption isotherms allow to designate the adsorption mechanism, surface properties and to determine the sorption capacity of sorbates on sorbent [48]. For modeling the adsorption isotherms of Indigo carmine and Orange II on the synthesized Al-Fm MOF, non-linear equations of two-parameter isotherms of: Langmuir, Freundlich, Temkin and Dubinin Radushkevich were adopted and represented in Fig. 8. These curves made it possible to determine the parameters specific to these models recorded in Table 8.

Outcomes reported in Table 8 generally demonstrate that all these isotherm models can be utilized to elucidate adsorptions of Indigo carmine and Orange II on the Al-Fum MOF. However, the Temkin and Dubinin models Radushkevick are the ones who best describe these adsorptions thanks to their coefficients of determination R^2 which tend towards unity. The maximum monolayer coverage of Indigo carmine and Orange II on a heterogeneous surface of the Al- Fum MOF is justified once again, not only with the help of the adsorbed quantities of the Langmuir model (59.663 and 27.612 mg/g respectively) sufficiently high; but also, by the values of R_L (separation factor) between 0 and 1 (0.001 and 0.024 L/mg). The outcomes are in comply with those acquired by Karmaka et *al.* in 2016, during their work on the adsorption of fluorine by the Al-Fum MOF [22]; thus, showing that the material has a high activity towards different pollutants. The inferior values of χ^2 and those of RSME and HYBRID error functions also demonstrate that the best models that best elucidate the adsorption isotherms of Indigo Carmine and Orange II are those of Temkin and Dubinin-Radushkevich. These interpretations are similar with the work of the research in sorption of reactive blue-19 based on activated carbon from cocoa pods [49]. The n values of the Freundlich constant are respectively equal to 1.639 and 0.8 for Indigo carmine and Orange II. They indicate in accordance with the literature data that the adsorption is favorable for both pollutants but better for Indigo carmine. These results also suggest that the adsorption process would occur on heterogeneous surfaces, with a non-uniform distribution of heat of sorption on this surface. This hypothesis would reflect the fact that the heat of sorption is not uniform on the surface, which would affirm that this phenomenon also presents a multi-layer adsorption: physisorption. With respect to the adsorption of Indigo carmine by Al-Fum MOF [50].

The Temkin model's positive adsorption energy values indicate that the adsorption process is exothermic. Adsorption energy estimates derived from the Dubinin-Radushkevich model (12.909 and 9.128 kJ/mol) being between 8 and 16 kJ/mol for the adsorptions of both pollutants, suggest that the favorable mechanism for this adsorption phenomenon is of physiochemical type.

3.4. Experimental design on sorption of Indigo Carmine and Orange II

3.4.1. Development of the regression equation model

Centered composite designs were used to develop a correlation betwixt the adsorption variables of Indigo Carmine and Orange II by Al-Fum MOF. These complete experimental designs along with their responses are presented in Table 9.

Table 9 shows that the adsorbed Indigo Carmine amounts are located between 0.757 and 13.260 mg/g. Tests 15 to 20 at central point were exploited to measure experimental error. The adsorbed Orange II amounts are located between 1.249 and 11.611 mg/g. Based on the sum of squares of the sequential models, the higher order polynomials were used for the choice of the latter, where the additional terms were significant and without models being biased [51]. For all these modelings, quadratic model was used, as proposed by software. Eqs. 5 and 6 in coded variables represent the regression models where the responses are the adsorbed amount as a function of the experimental variables.

$$(CI) = 7.34 + 3.54x_1 - 2.20x_2 - 0.88x_3 - 1.13x_1x_2 + 0.26x_1x_3 + 0.54x_2x_3 - 3.56x_1^2 + 1.84x_2^2 + 0.08x_3^2 \quad (5)$$

$$Y\ (OII) = 5.51 + 1.01x_1 - 1.84x_2 - 2.12x_3 + 0.15x_1x_2 - 0.34x_1x_3 + 1.06x_2x_3 + 0.15x_1^2 - 0.77x_2^2 + 0.22x_3^2 \quad (6)$$

These models could therefore be used to predict the responses based on the variables x_1, x_2 and x_3. The performance of the developed models was evaluated on the basis of the correlation coefficients R^2. Dependent upon methodology exploited, a model is validated for a value of the correlation coefficient $R^2 \geq 75$ %. In the current study, these values of R^2 were 95.57 and 97.38 respectivement for Indigo Carmine and Orange II with the adjusted R^2 values of 91.58 and 95.03.

These results indicate a good agreement between experimental and predicted data [52]. In view of these results, it is plausible to conclude

Table 8
Adsorption isotherms parameters of Al-fum MOF onto Indigo Carmine and Orange II.

N	Models	Constants	Values	R^2	RSME	χ^2	HYBRID	ARE	EABS
Indigo Carmine									
1	**Langmuir**	Q_e (mg/g)	59.663	0.910	5.785	2.380	120.993	19.231	11.632
		K_L (L/mg)	0.024						
2	**Freundlich**	K_f (L/mg)	2.980	0.854	7.395	3.419	174.647	23.811	15.582
		n	1.639						
3	**Temkin**	K_T (L/mg)	0.188	0.963	4.137	1.011	37.838	11.380	8.789
		b_T (J/mol)	169.349						
4	**DRK**	Q_{max} (mg/g)	45.369	0.977	3.187	0.743	29.223	9.500	6.236
		K (L/mg)	0.003						
		E (kJ/mol)	12.909						
Orange II									
1	**Langmuir**	Q_e (mg/g)	27.612	0.791	5.928	3.954	347.290	48.879	11.419
		K_L (L/mg)	0.001						
2	**Freundlich**	K_f (L/mg)	0.325	0.852	5.599	3.290	225.348	39.385	10.865
		n	0.854						
3	**Temkin**	K_T (L/mg)	0.098	0.974	2.642	0.449	15.319	9.488	5.187
		b_T (J/mol)	143.853						
4	**DRK**	Q_{max} (mg/g)	50.420	0.949	3.490	1.385	73.088	22.667	6.870
		K (L/mg)	0.006						
		E (kJ/mol)	9.128						

Table 9
Experimental matrix of a centered composite design of the optimization of sorption of Indigo Carmine and Orange II onto the Al- Fum MOF.

No.	Concentration of the pollutant (mg/L)	Mass (mg)	pH	Quantity adsorbed Q (mg/g) Indigo Carmine		Quantity adsorbed Q (mg/g) Orange II	
				Observed values	Predicted values	Observed values	Predicted values
1	20	25	3	4.398	4.909	9.117	8.927
2	100	25	3	33.437	34.723	22.921	23.311
3	20	125	3	1.635	1.685	3.352	2.844
4	100	125	3	6.824	5.997	15.638	15.832
5	20	25	8	0.575	1.554	3.591	3.260
6	100	25	8	11.315	11.417	3.930	4.301
7	20	125	8	0.619	0.484	1.249	1.400
8	100	125	8	6.206	5.846	2.981	3.034
9	20	75	5.5	1.635	0.230	3.777	4.656
10	100	75	5.5	6.519	7.318	7.002	6.671
11	60	25	5.5	13.260	11.380	6.145	6.582
12	60	125	5.5	5.711	6.983	2.797	2.907
13	60	75	3	8.317	8.297	7.0557	7.846
14	60	75	8	7.131	6.545	3.857	3.613
15	60	75	5.5	6.681	7.337	5.752	5.511
16	60	75	5.5	7.344	7.337	5.520	5.511
17	60	75	5.5	6.888	7.337	5.786	5.511
18	60	75	5.5	7.352	7.337	5.719	5.511
19	60	75	5.5	7.256	7.337	5.679	5.511
20	60	75	5.5	7.285	7.337	5.706	5.511

Legend : x_1 : Concentration of the dye solution (mg/L); x_2 : mass of Al-Fum MOF (mg); x_3 : pH of the solution; Val. Exp.: Experimental value and Val. Exp.: Predicted value.

without risk of error that approximately 95 % of these results can be described by suggested models.

3.4.2. Analysis of variance

In Eqs. 6 and 7, a positive coefficient value would indicate a positive effect on both Q_e and R, whereas a negative coefficient value would indicate a negative effect on these same values.

From this point of view, regarding the adsorption of Indigo Carmine (Eq. 5), it is observed that the concentration, the interactions between concentration and pH, between mass and pH, as well as the quadratic effects of mass and pH positively influence the amount of Indigo Carmine adsorbed by the Al-Fum MOF, while the other coefficients and other interactions influence it negatively.

Concerning the adsorption of Orange II (Eq. 6), it is observed that the pH, the concentration, the interactions between pH and concentration, between concentration and mass, as well as the quadratic effects of pH positively influence the amount of Orange II adsorbed by the Al-Fum MOF, while the other coefficients and other interactions influence it negatively.

ANOVA of the quadratic models was carried out to appraise significance of such effects, and the results are shown in Table 10. The model terms are considered significant if the probability value (*P*-value) is less than 0.05, and not significant if the *P*-value is more than 0.05 [53]. In the present work, although most of the parameters studied have a significant influence on the adsorption phenomenon, pH is the coefficient in linear and quadratic terms that has a greater influence as indicated by *P*-values less than 0.05 [54] for both Indigo Carmine and Orange II adsorption. This observation could be justified by the fact that pH influences both the surface of the material and the behavior of pollutants in solution.

Table 10
Probability-value values as a function of the different models of Indigo Carmine and Orange II adsorption on Al-Fum MOF.

Model	Factors	Quantity adsorbed < 0.0001	
		Indigo carmine	Orange II
Linear term	x_1: Conc. Pollutant	< 0.0001	0.0001
	x_2 : Mass	< 0.0001	< 0.0001
	x_3 : pH	0.0241	< 0.0001
Interactions	$x_1 x_2$	0.0123	0.4388
	$x_1 x_3$	0.4933	0.0951
	$x_2 x_3$	0.1751	0.0002
Quadratic term	x_1x_1	0.0002	0.6377
	x_2x_2	0.0150	0.0344
	x_3x_3	0.8972	0.5012

significant p value ($p < 0.05$).

3.4.3. Response surfaces, and main effect of factors on each adsorption response

The obtained models are presented in Fig. 9. These diagrams show the reciprocal influences, as well as the interdependencies between pH, concentration and mass of adsorbent on the adsorbed amounts of Indigo Carmine and Orange II in aqueous solution for 50 and 80 min, respectively. Fig. 9 in its sub-parts (a), (b) and (c) shows that the adsorbed quantity remains maximal (represented by the red part of the response surface) for Indigo Carmine solutions characterized by a high concentration (close to 100 mg/L), an acid pH (near 4) brought into contact with a relatively small quantity of Al-Fum MOF (around 25 mg). This could be explained once again by the affinity between the material and the adsorbate in an acidic medium evoked by the pH_{PZC}, and by the absence of the bulk at the contact surfaces of the material when it is in small quantity. By analogy with Indigo Carmine, sub-parts (d), (e) and (f) of Fig. 9, present similarities for the adsorption of Orange II on the Al-Fum MOF; with the only difference that the ideal pH in this adsorption is 3.

3.4.4. Validation of emperical model

The optimization of adsorption parameters was carried out using the software "*Statgraphics version 18.0*". The results are presented in Table 11.

The values of the experimental adsorbed quantities were obtained in both cases by carrying out the experiments under the conditions predicted in Table 11. It generally follows that, with comparatively minor errors (less than 2 %) between the expected and experimental values, the experimental values obtained agree with those predicted by these two models.

3.5. Regeneration and reuse of material

One significant issue influencing an adsorbent's viability for real-world use is its capacity for regeneration. In order to examine the regeneration capabilities of Al-Fum MOF toward the two dyes,

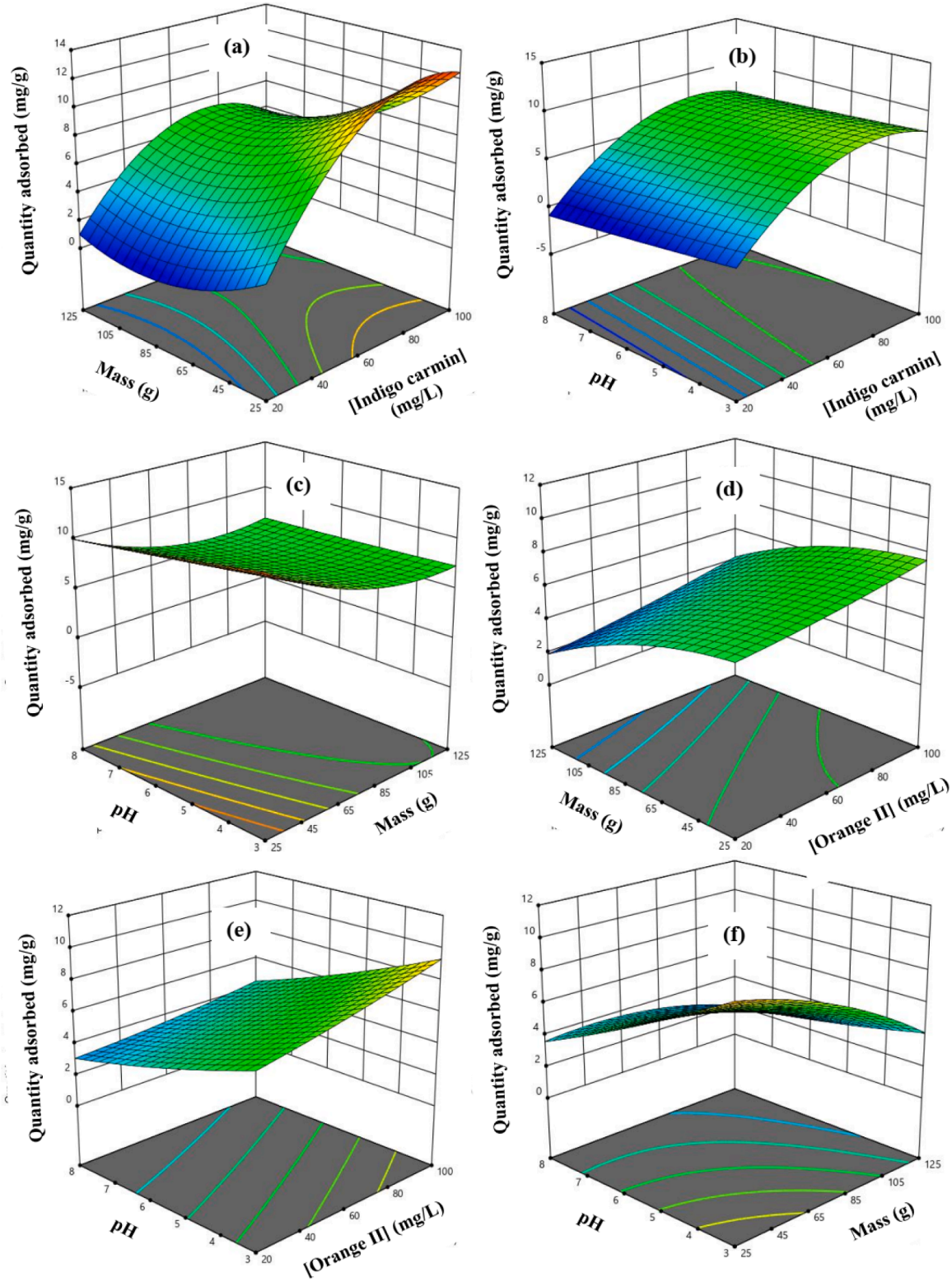


Fig. 9. Three-dimensional surface responses, and effects of the studied Qe factors for sorption of Indigo Carmine and Orange II in the Al-Fum MOF.

adsorption-desorption experiments were carried out. Fig. 10 illustrates the small decrease in the adsorbed quantity following five adsorption-desorption cycles.

The coupled histograms in Fig. 10 clearly show that Indigo Carmine and Orange II could be efficiently desorbed after centrifugation with distilled water followed by moderate heating (75°C); and that the Al-Fum MOF could be efficiently separated from the reaction medium and then regenerated.

This figure shows that after the first reuse, the adsorbed amount of Indigo Carmine on the Al-Fum MOF drops considerably from 32.90 to 11.50 mg/g; while that of Orange II drops from 21.67 to 6.11 mg/g. But after five successive reuse cycles, this variation gap decreases although slightly more considerable for Indigo Carmine. It drops from 11.50 to 7.01 mg/g for Indigo Carmine and from 6.11 to 4.80 mg/g for Orange II.

Table 11
Model validation for Indigo Carmine and Orange II adsorption in Al-Fum MOF.

	Optimal conditions						
	Answers	**Conc. (mg/L)**	**Mass (mg)**	**pH**	**Predicted values**	**Experimental values**	**Percentage error**
Indigo carmine	Amount adsorbed (mg/g)	84.7	25.0	3	34.2	33.8	**1.11 %**
Orange II	Amount adsorbed (mg/g)	100	25.0	3	23.3	22.9	**1.77 %**

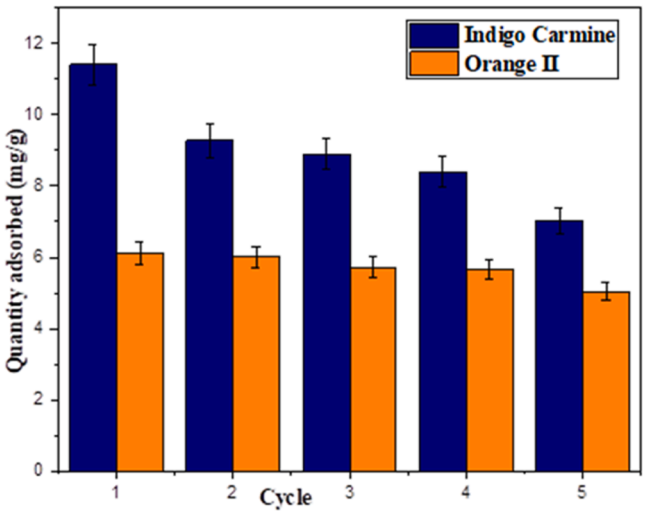


Fig. 10. Adsorption capacity of Al-Fum MOF on Indigo Carmine and Orange II after recycling.

In view of these results, the considerable decrease in the quantities adsorbed during the first reuses in these two cases would consider either a loss of the specific surface of the adsorbent due to phenomena such as: sintering caused by the leaching phenomenon during centrifugation, attrition due to chemical transformations of active sites into non-active sites following chemical reactions. Or by the inaccessibility of certain active sites previously occupied by the adsorbents and remaining unregenerated during reactivation. Following these remarks, it would once again be plausible to affirm that physiochemical interaction is the major process governing this adsorption and that the energy supplied during the treatment would be insufficient to break the new bonds formed.

The stability of the material observed on the adsorbed quantities after these first reuses would therefore be due to much more physical adsorptions and desorptions favored by the fragility of the van der waals bonds. However, the reduction in the adsorbed quantity of Indigo Carmine by the material at the end of fifth cycle reveals an average loss of activity of approximately 70 %, so the material would remain almost inactive at the end of the eighth cycle used. By analogy for the Orange II, the rate of loss of the adsorbent activity of the material during the first five cycles would be approximately 79 % and the latter will experience almost zero activity during its seventh reuse.

3.6. Study of plausible adsorption mechanisms

It is important to note that these reactions are possibilities of the multiple possible variants that would justify the adsorption process of IC and OII with respect to Al-Fum MOF. Depending on the reaction medium, it appears primarily that non-covalent interactions would be the most involved during this process; it remains less that some covalent interactions have also been listed. Covalent interactions are those involving more dispersed variations of electromagnetic interactions between molecules or atoms within a molecule. They can be classified into different categories including: electrostatic effects and pi (π) effects. Electrostatic interactions are those that involve not only the attraction of ions or molecules with permanent charges of opposite signs called Van der Waals; notably those of Keersom [55]. They also involve molecules with a charge localized on a particular atom: case of hydrogen bonds between a hydrogen atom and heteroatoms (O, N in this case). Pi (π) effects are generally those associated with molecular interactions with the π systems of conjugated molecules such as benzene [56]. In this study, those encountered here are pi-pi interactions: between benzene rings and double bond and n- π interactions between benzene rings and positively charged oxygen atoms (induced dipoles). As for covalent interactions, those highlighted are called dative. They are revealed during the complexation between electron-rich atoms of the different pollutants (ligands) and the central metal of the bifunctional material, thus forming coordination complexes. The different mechanisms are represented in turn in Figs. 11 and 12.

3.6.1. Plausible mechanisms of Indigo Carmine with respect to Al-Fum MOF ($pH < pH_{PZC}$)

The proposed mechanisms are made on the basis of the possible affinities between atoms depending on their states in the reaction medium. We therefore have the following proposals in Fig. 11 for the case of Indigo Carmine.

3.6.2. Plausible mechanisms of Orange II with respect to Al-Fum MOF ($pH < pH_{PZC}$)

The proposed mechanisms are made on the basis of the possible affinities between atoms depending on their states in the reaction medium. We therefore have the following proposals in Fig. 12 for the case of Orange II.

Table 12 presents some results from the literature on the adsorption of these two dyes. The results of the comparative study between the results of this work and those of previous works under similar experimental conditions are in agreement. It is noted that Al-Fum MOF is an eligible and effective material in the removal of organic dyes, including Indigo Carmine and Orange II. From this comparative study, it emerges first of all that the quantity of Indigo Carmine adsorbed by Al-Fum MOF (33.8 mg/g) is considerable than those of materials such as: TiO_2 "600 °C", TiO_2 "Fluka" and Lamellar Hydroxide ($ZnAlCO_3$); although this value is lower than that of Lamellar Hydroxide (ZnAlC500). From these results, it also emerges that the quantity of Orange II adsorbed by Al-Fum MOF (22.9 mg/g) is greater than that of certain other materials such as: P.brutia PCB-05 M (20.4 mg/g), TiO_2 PC25 (1.6 mg/g). This value is also lower compared to that of many other materials such as JB AC activated carbon (i.e. 349.9 mg/g for an initial volume of 1000 mL of solution).

The Al-Fum MOF stands out as a promising adsorbent for the removal of organic pollutants such as Indigo Carmine and Orange II. With an adsorption capacity of 33.8 mg/g for Indigo Carmine and 22.9 mg/g for Orange II, this material demonstrates notable effectiveness under specific experimental conditions.

MOFs, including Al-Fum MOF, are known for their highly adjustable pore structure, which enables them to target specific pollutants based on size and shape. The large specific surface area of Al-Fum MOF contributes to its high adsorption capacity, allowing for effective interaction with pollutant molecules. Also, MOF adsorbents can be designed to exhibit high chemical stability, which is crucial for practical applications where conditions may vary.

As a Limitation, compared to some other adsorbents such as Lamellar

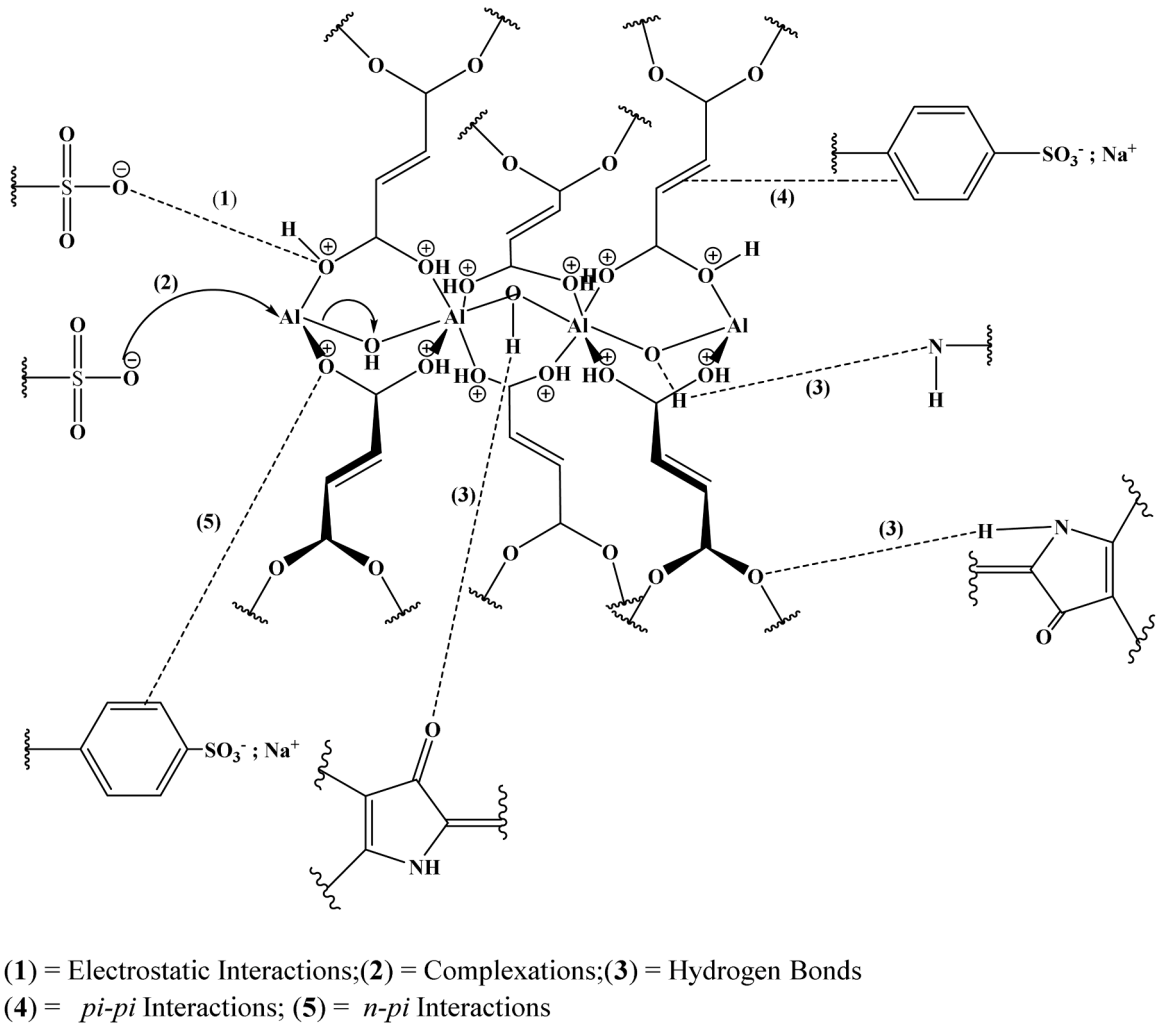


Fig. 11. Possible adsorption mechanisms of Indigo Carmine on Al-Fum MOF.

hydroxide (ZnAlC500) for Indigo Carmine or Activated carbon (JB AC) for Orange II, Al-fum MOF exhibits moderate adsorption capacities. This may require larger quantities of material to achieve the same levels of purification. Also, the synthesis and large-scale production of MOFs can be expensive and complex, which may limit their applicability in certain industrial or environmental contexts.

4. Conclusion

This study investigated the adsorption of Orange II and Indigo Carmine dyes on a metal-organic framework-based material (Al-Fum MOF) in aqueous solution. The results obtained from the characterization show that the synthesis was successfully carried out presenting a specific surface area of 1025 m^2/g with a crystalline structure. The adsorption kinetics are well described by the pseudo-second-order model with a χ^2-test of 0.175 for indigo carmine as well as the Elovich model for Orange II with a χ^2-test of 0.171, and the adsorption energetic values suggest a physicochemical interaction mechanism. These results are promising for the practical application of Al-Fum MOF in industrial wastewater treatment. Recyclability studies of the adsorbent show that deactivation depends on the pollutant, which is around 40 % for Indigo Carmine and 20 % for Orange II after five cycles of use, highlighting the good stability of the Al-Fum MOF material. However, it is important to note that the efficiency of the Al-Fum MOF decreases considerably after the first use, which requires regular regeneration of the material. To improve the value of this work and guide future research, it would be interesting to conduct additional studies on the stability and hardness of the Al-Fum MOF, as well as on the adsorption and regeneration mechanisms. In addition, it would be useful to conduct additional analyses, such as XRD and FTIR, on the material after use to evaluate the structural and chemical changes that might occur during the adsorption process. This study contributes to the advancement of knowledge on adsorbent materials for wastewater treatment and highlights the potential of Al-Fum MOF for practical applications. Also, Al-fum MOF offers promising prospects for the treatment of contaminated water due to its adjustable structure and high specific surface area. Further research on optimizing its synthesis, improving its adsorption capacity, and reducing production costs could broaden its practical applicability.

Funding

This research received no external funding.

CRediT authorship contribution statement

Albert-Yannick-Steve Mbega: Writing – original draft, Data curation. **Cyrille Ghislain Fotsop:** Methodology, Conceptualization. **Donald Raoul Tchuifon Tchuifon:** Writing – original draft, Supervision, Software, Formal analysis, Data curation, Conceptualization. **Paul Alain Nanssou Kouteu:** Software, Investigation. **Frank Dorinel Solefack Feudjio:** Writing – original draft, Software, Investigation. **Aurelien Bopda:** Writing – review & editing, Writing – original draft, Software,

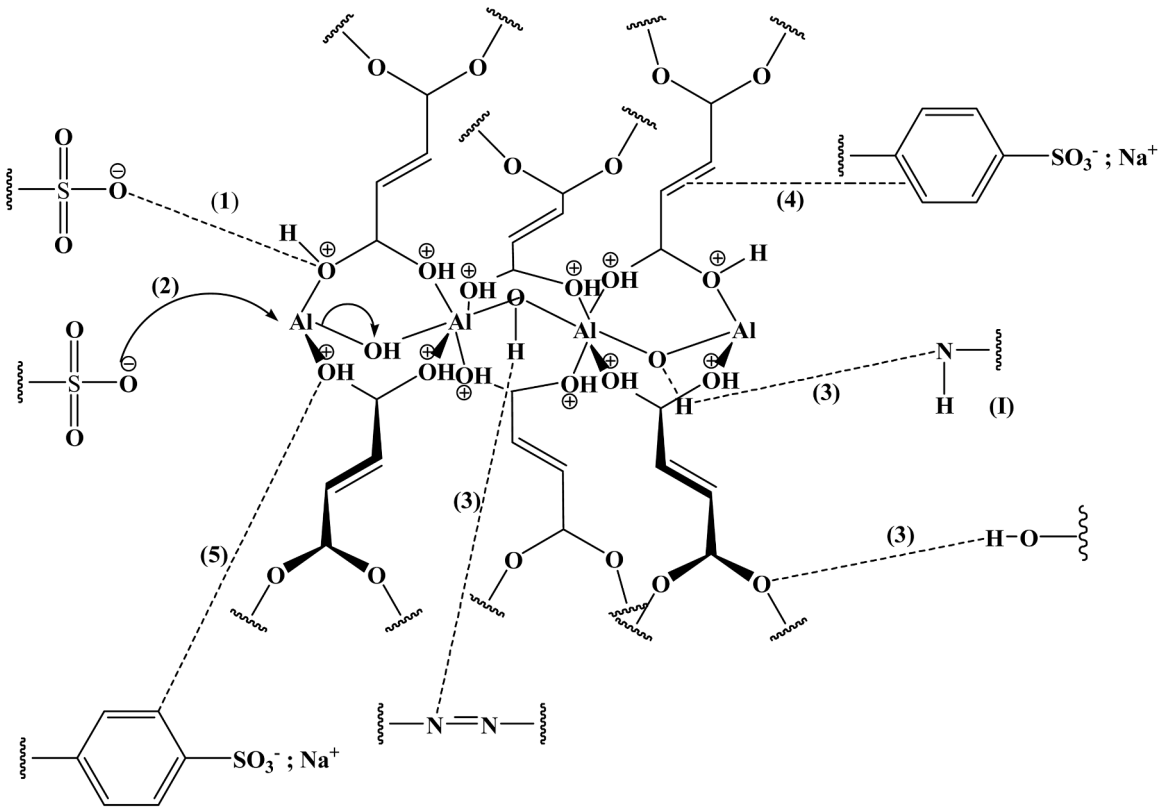


Fig. 12. Possible adsorption mechanisms of Orange II on Al-Fum MOF.

Table 12
Comparative analysis with previous works.

Adsorbent	pollutant	Q_e (mg/g)	Experimental conditions C_0 (mg/L); m_o (g); V_0 (mL)	Reference
Lamellar hydroxide (ZnAlC500)	Indigo Carmine	526.6	200; 0.01; 50	[57]
Lamellar hydroxide ($ZnAlCO_3$)	Indigo Carmine	21.7	100; 0.01; 50	
TiO_2 "Fluka"	Indigo Carmine	3.4	20; 2; —	[58]
TiO_2 "600 °C"	Indigo Carmine	9.1	20; 2; —	
Al-Fum MOF	Indigo Carmine	**33.8**	**85; 25; 20**	**This work**
Activated carbon (JB AC)	Orange II	349.9	2800; 16; 1000	[59]
TiO_2 (PC25)	Orange II	1.6	35; 25; 60	[60]
Activated carbon (capV1)	Orange II	170.0	35; 2; 1000	
P.brutia (PCB-0M)	Orange II	32.7	100; 50; 50	[61]
P.brutia (PCB-05M)	Orange II	20.4	20; 50; 50	
Al-Fum MOF	**Orange II**	**22.9**	**100; 25; 20**	**This work**

Data curation. **Omirserik Baigenzhenov:** Writing – review & editing, Writing – original draft, Validation. **Ahmad Hosseini-Bandegharaei:** Writing – review & editing, Writing – original draft, Validation, Supervision, Software, Project administration, Methodology, Data curation.

Declaration of competing interest

The authors declare that they have no known competing financial interests or personal relationships that could have appeared to influence the work reported in this paper.

Acknowledgment

The authors are thankful to all members of the Research Team of the University of Douala, Cameroon, particularly Mrs. FOKO Roland and Dongmo Dave Sanchez.

Data availability

The authors declare that data supporting the funding of this study are available within the article.

Reference

[1] Y. Rakcho, A. Naboulsi, T. Bouzid, Y. Abouliatim, A. Benhammou, A. Abourriche, Et.J. Alami, Treating waste with waste: treatment of textile wastewater using upcycled food waste as a pore-forming agent in the fabrication of ceramic membranes employing DOE/FFD design, Waste Manag. 190 (2024) 632–643.
[2] Y. Rakcho, M. Baidou, A. Naboulsi, A. Bouazizi, M. Mouiya, H. Sehaqui, Et. Y. Abouliatim, Fabrication of low-cost ceramic nanofiltration membrane from

natural resources for the removal of cationic and anionic dyes: experimental and DFT investigation, Chem. Eng. 505 (2025) 1159779.
[3] M. Bellaj, H. Yazid, K. Aziz, Et.A. Regti, Eco-friendly synthesis of clay-chitosan composite for efficient removal of alizarin red S dye from wastewater: A comprehensive experimental and theoretical investigation, Environ. Res. 247 (2024) 1118352.
[4] N.A.G. Nche, A. Bopda, D.R.T. Tchuifon, C.S. Ngakou, I.H.T. Kuete, A.S. Gabche, Removal of paracetamol from aqueous solution by adsorption onto activated carbon prepared from rice husk, J Chem Pharm Res 9 (2017) 56–68.
[5] D.R.T. Tchuifon, C.G. Fotsop, S.G.M. Mafo, F.D.S. Feudjio, S.D.M. Dongmo, N.A. G. Nche, Unveiling the photocatalytic activity of Cu/Fe2O3@ gC3N4 nanosheet as an efficient Fenton-like catalyst for reactive blue 19 removal: optimization and kinetics studies, Hybrid Adv. (2025) 100424.
[6] R. Al-Tohamy, S.S. Ali, F. Li, K.M. Okasha, Y.A.G. Mahmoud, T. Elsamahy, H. Jiao, Y. Fu, J. Sun, A critical review on the treatment of dye-containing wastewater: ecotoxicological and health concerns of textile dyes and possible remediation approaches for environmental safety, Ecotoxicol. Environ. Saf. 231 (2022) 113160.
[7] M.E. Ristea, O. Zarnescu, Indigo carmine: between necessity and concern, J. Xenobiot. 13 (2023) 509–528.
[8] A. Yadav, A. Kumar, P.D. Dwivedi, A. Tripathi, M. Das, In vitro studies on immunotoxic potential of orange II in splenocytes, Toxicol. Lett. 208 (2012) 239–245.
[9] M. de Keijzer, M.R. van Bommel, R.H.D. Keijzer, R. Knaller, E. Oberhumer, Indigo carmine: understanding a problematic blue dye, Stud. Conserv. 57 (2012) S87–S95.
[10] F. Akter, Y. Dong, Investigation of removing orange II azo dye from wastewater through an oxidation process, Appl. Water Sci. 14 (2024) 1–13.
[11] S.G.M. Mafo, D.R.T. Tchuifon, F.H.K. Djioko, P.A.N. Kouteu, C.G. Fotsop, S.D. M. Dongmo, G. Doungmo, N.A.G. Nche, Unravelling the efficiency removal of 2, 4-dinitrophenol on coconut shell biomass-derived activated carbons theoretical and experimental investigation, Biomass Convers. Biorefin. (2024) 1–21.
[12] S.A. Benedoue, J.N. Ndi, M. Ge, Z. Tian, C.B.D. Nguela, H. Tong, A. Lo Presti, M. Antonietti, H.M. Ngomo, C.M. Pelicano, Controllable acid activation of sulfur-doped carbon nitride enables enhancement in photocatalytic indigo carmine degradation performance, ACS Sustain. Chem. Eng. 12 (2024) 16809–16816.
[13] A. B. Debina, S.N. Eric, D. Fotio, K. Tamo, D.Y. Lemankreo, A.N. Rahman, Adsorption of indigo carmine dye by composite activated carbons prepared from plastic waste (PET) and banana pseudo stem J. Mater. Sci. Chem. Eng. 8 (2020) 39–55.
[14] Y. Sun, L. Chen, F. Zhang, D. Li, H. Pan, J. Ye, First-principles studies of HF molecule adsorption on intrinsic graphene and Al-doped graphene, Solid State Commun. 150 (2010) 1906–1910.
[15] L.T. Nanganoa, J.M. Ketcha, J.N. Ndi, Kinetic and equilibrium modeling of the adsorption of amaranth from aqueous solution onto smectite clay, Res. J. Chem. Sci. 4 (2014) 7–14.
[16] F.A. Awadallah, F. Hillman, S.A. Al-Muhtaseb, H.K. Jeong, On the nanogate-opening pressures of copper-doped zeolitic imidazolate framework ZIF-8 for the adsorption of propane, propylene, isobutane, and n-butane, J. Mater. Sci. 54 (2019) 5513–5527.
[17] E.C. Nnadozie, P.A. Ajibade, Isotherm, kinetics, thermodynamics studies and effects of carbonization temperature on adsorption of Indigo Carmine (IC) dye using C. odorata biochar, Chem. Data Collect. 33 (2021) 100673.
[18] P. Xiong, H. Zhang, G. Li, C. Liao, G. Jiang, Adsorption removal of ibuprofen and naproxen from aqueous solution with Cu-doped Mil-101 (Fe), Sci. Total Environ. 797 (2021) 149179.
[19] S.G.M. Mafo, P.A.N. Kouteu, D.R.T. Tchuifon, C.G. Fotsop, M.Z. Mve, G.T. Kenda, A. Bopda, I.T.H. Kuete, S.C. Ngakou, N.A.G. Nche, M.R. Mouangue, S.G. Anagho, Low-cost magnetic carbons-based rubber seed husks materials for highly efficient removal for reactive black 5 and reactive blue 19 textile dyes from wastewater, Int. J. Environ. Anal. Chem. 105 (2025) 701–725.
[20] M.S. Tehrani, R. Zare-Dorabei, Highly efficient simultaneous ultrasonic-assisted adsorption of methylene blue and rhodamine B onto metal organic framework MIL-68 (Al): central composite design optimization, RSC Adv. 6 (2016) 27416–27425.
[21] X. Liu, W. Gong, J. Luo, C. Zou, Y. Yang, S. Yang, Selective adsorption of cationic dyes from aqueous solution by polyoxometalate-based metal–organic framework composite, Appl. Surf. Sci. 362 (2016) 517–524.
[22] J. Dechnik, C. Janiak, S. De, Aluminium fumarate metal-organic framework: a super adsorbent for fluoride from water, J. Hazard. Mater. 303 (2016) 10–20.
[23] E. Moumen, L. Bazzi, S. El Hankari, Aluminum-fumarate based MOF: a promising environmentally friendly adsorbent for the removal of phosphate, Process Saf. Environ. Prot. 160 (2022) 502–512.
[24] E. Alvarez, N. Guillou, C. Martineau, B. Bueken, B. Van de Voorde, C.P. Le Guillouzer, F. Nouar, F. Taulelle, D. deVos, J.S. Chang, K.H Cho, N. Ramsahye, T. Devic, M. Daturi, C. Serre, The structure of the aluminum fumarate metal–organic framework A520, Angew. Chem. Int. Ed. 54 (2015) 3664–3668.
[25] Y.S. Ho, G. McKay, Pseudo-second order model for sorption processes, Process Biochem. 34 (1999) 451–465.
[26] S.H. Chien, W.R. Clayton, Application of Elovich equation to the kinetics of phosphate release and sorption in soils, Soil Sci. Soc. Am. J. 44 (1980) 265–268.
[27] A. Marszałek, G. Kamińska, N.F.A. Salam, Simultaneous adsorption of organic and inorganic micropollutants from rainwater by bentonite and bentonitecarbon nanotubes composites, J. Water Process Eng. 46 (2022) 102550.
[28] A. Bopda, C.G. Fotsop, G.T. Kenda, D.R.T. Tchuifon, F.F. Mache, K.L.T. Nguena, G. Doungmo, N.G. Ndifor-Angwafor, K.S. Ghosh, A. Hosseini-Bandegharaei, Investigating the uptake of brilliant blue FCF and orange II dyes from aqueous solution onto a porous Al-based MOF sorbent (CAU-10-H), Inor. Chem. Com. 178 (2) (2025), https://doi.org/10.1016/j.inoche.2025.114560.
[29] A.L. Djoumbissie, D.R.T. Tchuifon, A.D. Cyrille, I.H.T. Kuete, D. Giscard, T.D. A. Clovis, J. Ngoune, Kinetic and isotherm studies of the adsorption phenacetin onto two copper porous coordination compounds: nonlinear regression analysis, J. Chem. 2022 (2022) 2828860.
[30] A.O. Dada, A.P. Olalekan, A.M. Olatunya, O.J.I.J.C. Dada, F. Langmuir, Temkin and Dubinin–Radushkevich isotherms studies of equilibrium sorption of Zn^{2+} unto phosphoric acid modified rice husk, IOSR J. Appl. Chem. 3 (2012) 38–45.
[31] F.H.K. Djioko, C.G. Fotsop, G.K. Youbi, S.C. Nwanonenyi, E.E. Oguzie, C.A. Madu, Efficient removal of pharmaceutical contaminant in wastewater using low-cost zeolite 4A derived from kaolin: experimental and theoretical studies, Mat. Chem. Phys. 315 (2024), https://doi.org/10.1016/j.matchemphys.2024.128994.
[32] M.I. Temkin, Kinetics of ammonia synthesis on promoted iron catalysts, Acta Physiochim. URSS 12 (1940) 327–356.
[33] M. Dong, H. Zhou, W. Liu, C. He, Activated carbon prepared from semi-coke as an effective adsorbent for dyes, Pol. J. Environ. Stud. 29 (2020) 1137–1142.
[34] D.R.T. Tchuifon, N.A.G. Nche, A. Bopda, S.G. Anagho, Modeling of phenol adsorption isotherm onto activated carbon by non-linear regression methods: models with three and four parameters, Desalin. Water Treat. 136 (2018) 199–206.
[35] D.C. Montgomery, Design and Analysis of Experiments, John wiley & sons, 2017.
[36] R. Azargohar, A.K. Dalai, Production of activated carbon from Luscar char: experimental and modeling studies, Microporous Mesoporous Mater. 85 (2005) 219–225.
[37] R. Azhdari, S.M. Mousavi, S.A. Hashemi, S. Bahrani, S. Ramakrishna, Decorated graphene with aluminum fumarate metal organic framework as a superior non-toxic agent for efficient removal of Congo Red dye from wastewater, J. Environ. Chem. Eng. 7 (2019) 103437.
[38] D.R.T. Tchuifon, L.K.T. Nguena, G. Doungmo, S.G.M. Mafo, F.D.S. Feudjio, C. G. Fotsop, Pyrolysis kinetics-dependent suitability of Al-based MOFs (CAU-10) for controlling amorphous γ-Al2O3 generation, Chem. Thermo. Ther. Anal. 18 (2025), https://doi.org/10.1016/j.ctta.2025.100175.
[39] L.R. MacGillivray, Metal-Organic Frameworks: design and Application, John Wiley & Sons, 2010.
[40] S. Karmakar, S. Bhattacharjee, S. De, Aluminium fumarate metal organic framework incorporated polyacrylonitrile hollow fiber membranes: spinning, characterization and application in fluoride removal from groundwater, Chem. Eng. J. 334 (2018) 41–53.
[41] R.M. Abdelhameed, M. Taha, H. Abdel-Gawad, B. Hegazi, Amino-functionalized Al-MIL-53 for dimethoate pesticide removal from wastewater and their intermolecular interactions, J. Mol. Liq. 327 (2021) 114852.
[42] G. Férey, Hybrid porous solids: past, present, future, Chem. Soc. Rev. 37 (2008) 191–214.
[43] T. Loiseau, C. Serre, C. Huguenard, G. Fink, F. Taulelle, M. Henry, G. Férey, A rationale for the large breathing of the porous aluminum terephthalate (MIL-53) upon hydration, Chem. Eur. J. 10 (2004) 1373–1382.
[44] G. Deffo, A.K. Tamo, C.G. Fotsop, H.H.B. Tchoumi, D.E.N. Talla, C.G. Wabo, M.C. N. Deussi, R.C.T. Temgoua, G. Doungmo, E. Njanja, I.K. Tonle, P. Puzari, C. Birkemeyer, E. Ngameni, Metal-organic framework-based materials: from synthesis and characterization routes to electrochemical sensing applications, Coor. Chem. Rev. 536 (2025), https://doi.org/10.1016/j.ccr.2025.216680.
[45] F.H.K. Djioko, C.G. Fotsop, G.K. Youbi, S.C. Nwanonenyi, C.A. Madu, E.E. Oguzie, Unraveling the sorption mechanisms of ciprofloxacin on the surface of zeolite 4A (001) in aqueous medium by DFT and MC approaches, Appl. Surf. Sci. Adv. 19 (2024), https://doi.org/10.1016/j.apsadv.2023.100542.
[46] T.E. Khalil, H. Altaher, R. Abubeah, Adsorptive removal of Cu (II) ions by date pits: kinetic and equilibrium studies, Environ. Eng. Manag. J. 15 (2016) 151–159.
[47] Q. Hu, Z. Xu, S. Qiao, F. Haghseresht, M. Wilson, G.Q. Lu, A novel color removal adsorbent from heterocoagulation of cationic and anionic clays, J. Colloid Interface Sci. 308 (2007) 191–199.
[48] A.Z. Mekuiko, D.R.T. Tchuifon, P.A.N. Kouteu, C.G. Fotsop, C.S. Ngakou, H.I. T. Kuete, S.G. Anagho, Tailoring activated carbons based cocoa pods lignocellulosic materials for Reactive blue 19 adsorption: optimization, adsorption isotherm and kinetic investigation, Desalin. Water Treat. 300 (2023) 144–157.
[49] V.D.O. Sousa Neto, T.V. Carvalho, S.B. Honorato, C.L. Gomes, F.C.F. Barros, P. T. Freire, R.F. Nascimento, Coconut bagasse treated by thiourea/ammonia solution for cadmium removal: kinetics and adsorption equilibrium, Bioresource 7 (2012).
[50] K.L.T. Nguena, C.G. Fotsop, A. Bopda, D.R.T. Tchuifon, F.H.K. Djioko, A.M. S. Ngueabouo, C.A. Madu, F.I. Ezema, E.E. Oguzie, Unraveling the sorption mechanism of industrial dyes onto Zr-based MOFs: computational and experimental modelling for highly efficient removal, Mater. Adv. 6 (2024) 579–597, https://doi.org/10.1039/D4MA00818A.
[51] C.S. Ngakou, N.H. Manga, D.R.T. Tchuifon, S.G. Anagho, Optimisation of activated carbon preparation by chemical activation of ayous sawdust, cucurbitaceae peelings and hen egg shells using response surface methodology, Int. Res. J. Pure Appl. Chem 14 (2017) 1–12.
[52] J.N. Sahu, J. Acharya, B.C. Meikap, Optimization of production conditions for activated carbons from Tamarind wood by zinc chloride using response surface methodology, Bioresour. Technol. 101 (2010) 1974–1982.
[53] S.G.M. Mafo, D.R.T. Tchuifon, C.S. Ngakou, C.G. Fotsop, P.A.N. Kouteu, G. Doungmo, S.G. Anagho, Study of the degradation of Bezaktiv Brilliant Blue by the Fenton process using a prepared ferromagnetic activated carbon from rubber seed hull as heterogeneous catalyst, Desalin. Water Treat. 287 (2023) 200–213.
[54] E.H. Lee, S.R. Byrn, R. Pinal, The solution properties of mefenamic acid and a closely related analogue are indistinguishable in polar solvents but significantly different in nonpolar environments, J. Pharm. Sci. 101 (12) (2012) 4529–4539.

[55] M.F. Mabesoone, A.R. Palmans, E.W. Meijer, Solute–solvent interactions in modern physical organic chemistry: supramolecular polymers as a muse, J. Am. Chem. Soc 142 (2020) 19781–19798.
[56] E. Asadi, P. Haroonian, M. Ghaedi, A. Asfaram, Removal of tartrazine and indigo carmine with layered double hydroxide-modified graphite nanocomposite: isotherm, kinetics and response surface methodology (RSM) optimization, J. Mol. Liq. 402 (2024) 124769.
[57] S. Alahiane, S. Qourzal, M. El Ouardi, M. Belmouden, A. Assabbane, Y. Ait-Ichou, Adsorption and photocatalytic degradation of indigo carmine dye in aqueous solutions using TiO_2/UV/O_2), J. Mater. Environ. Sci 4 (2013) 239–250.
[58] B. Zohra, (2019). Activation of jujube kernels to obtain activated carbon.
[59] L. Lucarelli, V. Nadtochenko, D.J. Kiwi, Environmental photochemistry: quantitative adsorption and FTIR studies during the TiO_2-photocatalyzed degradation of orange II, Langmuir 16 (3) (2000) 1102–1108.
[60] L.S. Oliveira, A.S. Franca, Low-cost adsorbents from agri-food wastes, Food Sci. Technol.: New Res. (2008) 171–209.
[61] J.P.N. Tejeogue, R. Djakba, C.G. Fotsop, N. Dobe, S. Mouhamadou, B. Wangmene, M. Harouna, Systematic metronidazole adsorption performance onto montmorillonite clay: parametric study, process modelling and RSM optimisation, Resl. Chem. 14 (2025), https://doi.org/10.1016/j.rechem.2025.102153.